THE GROWTH OF EPITAXIAL GRAPHENE FOR TWO-DIMENSIONAL ELECTRONICS

A Thesis Submitted to
The Graduate School of Engineering and Sciences of
İzmir Institute of Technology
In Partial Fulfilment of the Requirements for the Degree of

MASTER OF SCIENCE

in Physics

By
Alnazir IBRAHIM

July 2015
İZMİR

We approve the thesis of **Alnazir IBRAHIM**

Examining Committee Members:

_____

Assist. Prof. Dr. Cem ÇELEBİ
Department of Physics, İzmir Institute of Technology

_____

Assist. Prof. Dr. Gökhan UTLU
Department of Physics, Ege University

_____

Assoc. Prof. Dr. A. Devrim GÜÇLÜ
Department of Physics, İzmir Institute of Technology

10 July 2015

_____

Assist. Prof. Dr. Cem ÇELEBİ
Supervisor, Department of Physics,
İzmir Institute of Technology

_____

Prof. Dr. Nejat BULUT
Head of the Department of
Physics

_____

Prof. Dr. Bilge KARAÇALI
Dean of the Graduate School of
Engineering and Sciences

ACKNOWLEDGEMENTS

I would like to express my gratitude to my advisor Assist. Prof. Dr. Cem Çelebi for his invaluable advice, guidance and encouragement throughout this study.

I would also like to thank my friends Erdi Kuşdemir, Dilce Özkendir and Damla Yeşilpınar for their encouragement, help and patience all along.

And last but not least, I am also grateful to my family for leading me to this stage and for their endless support during all of my life.

ABSTRACT

THE GROWTH OF EPITAXIAL GRAPHENE FOR TWO-DIMENSIONAL ELECTRONICS

Graphene is a fundamentally new type of 2D electronic material exhibits extraordinary properties. In this work, we used the thermal decomposition of SiC in vacuum principle to grow epitaxial graphene on Both C-face and Si-face SiC, that because epitaxial graphene is a reliable candidate for all kind of applications in 2D electronics and it has similar properties to carbon nanotube and graphene grown by exfoliation method, but it is more appropriate for the design of electronic device as it can be grown on wafer-sized scale. We review the physical and electronic properties of graphene and what's makes it different when compare to the ordinary semiconductors. Since the interest in graphene increases as a perfect candidate for future electronics applications, many methods are used to synthesis graphene. We give a brief review to several methods used to produce graphene.

For electronic device applications, graphene should be grown in a high homogeneity, uniformity and with low growth rate. Therefore the growth rate graphene should be controlled to get high homogeneity and uniformity.

Raman spectroscopy considers a quick way to detect the presence of graphene, determine the number of the layers and to check the defects in the grown layer. At the wavelength of 514 nm , Raman spectroscopy is used to investigate epitaxial graphene grown on both C-face and Si-face SiC with different parameters and to study the evolution and the proportionality of the grown layers with the time . Finally we used AFM to study the morphology of epitaxial graphene grown on SiC substrate. The morphology of graphene on C-face of SiC is compared with the one on Si-face of SiC.

ÖZET

İKİ BOYUTLU ELEKTRONİK AYGITLAR İÇİN EPİTAKSİYEL GRAFEN BÜYÜTÜLMESİ

Grafen, sıra dışı özelliklere sahip temel, yeni bir tür iki boyutlu malzemedir. Bu çalışmada, silisyum karbürün (SiC) hem C-yüzü hem Si-yüzü kullanılarak vakum ortamında termal buharlaştırma yöntemi kullanılarak grafen büyütülüldü. Epitaksiyel grafen, mekanik ayrıştırma yöntemiyle elde edilen grafen ve karbon nanotüplere benzer özellik gösterdiğinden 2 boyutlu elektronik uygulamalarda kullanılmak için iyi bir adaydır, hatta büyük boyutlarda büyütülebildiği için elektronik aygıtların tasarımı için daha uygundur. Grafenin fiziksel, elektronik ve onu diğer yarıiletkenlerden ayıran özelliklerini incelendi. Gelecekteki elektronik uygulamalar için mükemmel bir aday oluşu grafen üzerindeki ilgiyi artırdığından dolayı grafen sentezinde pek çok yöntem kullanılmaktadır. Bu çalışmamızda biz birkaç grafen büyütme metodu üzerinde yoğunlaşıldı.

Grafen elektronik aygıt uygulamalarında kullanabilmek için; yüksek saflıkta ve düşük büyütme hızlarında büyütülmelidir. Bu nedenle, yüksek homojenlikte tek katman grafen elde edebilmek için grafenin büyütme hızının kontrol edilmesi gerekmektedir.

Grafenin varlığı ve katman sayısı hakkında bilgi edinmenin en hızlı yolu Raman spektroskopisidir. Farklı parametrelerde epitaksiyel olarak hem silisyum hem de karbon yüzeyinde büyütülmüş grafendeki değişim Raman spektroskopisi ile incelenmiştir. Epitaksiyel olarak büyütülmüş grafenin yüzey karakterizasyonu atomik kuvvet mikroskopu (AFM) ile yapılmıştır

TABLE OF CONTENTS

LIST OF FIGURES

Figure **Page**

LIST OF TABLES

Table **Page**

CHAPTER 1

INTRODUCTION

Graphene is single layer of Carbon (C) atoms densely packed in a honeycomb crystal lattice. Due to its exceptional electrical, physical, and chemical properties, graphene has revolutionized the scientific frontiers in nanoscience and condensed matter physics. Expected as possible replacement for Silicon (Si) in micro-advance electronics, graphene has attracted more interest in many research groups around the world .The interest in graphene is increasing because graphene shows several unusual and unique properties including very low resistivity (high conductivity), integer quantum Hall effect at half-integer filling factor, anomalous Shubnikov–de Haas oscillation, high carrier mobility, and ballistic transport even at room temperature. Moreover, electrons and holes behave like massless Dirac fermions with a fraction of speed of light and reveal a pseudo-spin due to two C sub-lattices. These effects are theoretically well understood and explained in terms of linear energy momentum dispersion. The reported properties and application of graphene have opened up new opportunities for future devices and systems. The possibility to control electrical, thermal, optical, mechanical and magnetic properties of the graphene sheets specially by controlling the graphitization phenomena (carbonization rate), makes graphene a very attractive material from both scientific and technological point of views. Furthermore, graphene epitaxially grown on SiC wafer, by thermal dissociation of Si atoms from SiC surface shows very interesting properties. There are several techniques developed to grow graphene such as mechanical exfoliation method and intercalation method. The methods including chemical vapour deposition (CVD) and epitaxial growth of graphene on SiC substrate. Epitaxial growth of graphene on SiC substrate is the main topic of this thesis work while exfoliation, CVD and intercalation methods are briefly discussed as well.

Graphite consists of many carbon sheets, in which the atoms are bound to three neighbours in a honeycomb structure and are stacked in three dimensional regular orders. This structure of graphite implies three dimensional geometry. In 1940s many of the theoretical works suggested that if graphite treated as isolated layers, the layers might exhibit extraordinary electronic characteristics, (e.g, special conductivity) [1]. More than 60 years later, these predictions correctly proven and the isolated layers of

graphite revealed more fantastic properties, such as high carrier motilities (>$2x10^5$ $cm^2V^{-1}s^{-1}$ at electron densities of $2x10^{11}cm^{-2}$), exponential young modules, and large spring constant [1].The single layer of C atoms that have been isolated from graphite is referred to graphene. The term graphene uses only when we talk about individual layer (2D layer) of this structure as shown in Figure (1.1a) [1]. The definition of the term graphene is available since 1986; when Boehm.et.al recommended standardizing the term, while the end ``(ene)'' is used for fused polycyclic aromatic hydrocarbons. In general graphene is defined as a single layer of C atoms arranged in a hexagonal lattice, as illustrated in figure (1.1b). Its atomic structure can be wrapped into 0D fullerenes, rolled into 1D nanotube or stacked into 3D graphite to construct other allotropes of C atoms [25].

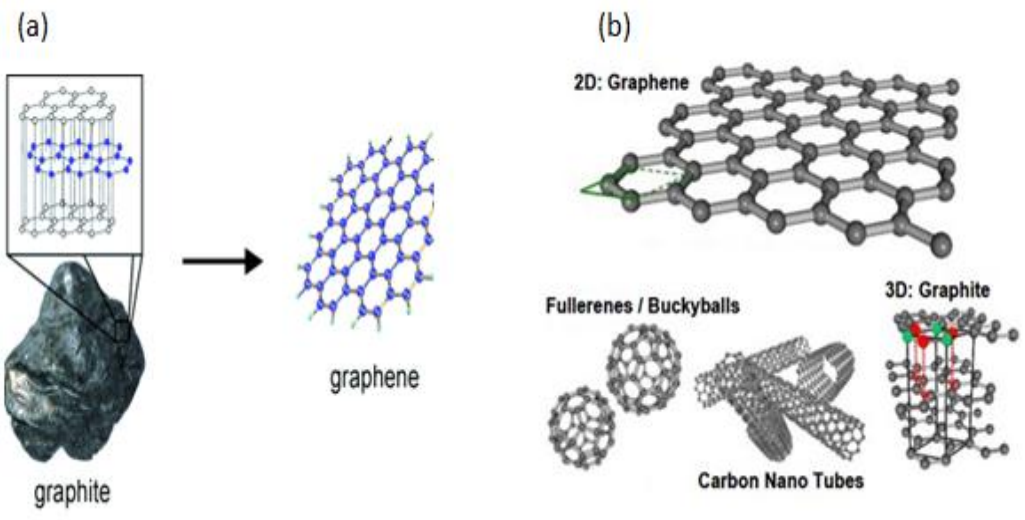

Figure 1.1. Mother of all graphitic forms. Graphene is 2D building material for Carbon material of all other dimensionalities and it can be wrapped up into 0D fullerenes, rolled up into 1D carbon nanotube or stacked into 3D graphite [2, 14].

Graphene lattice contains pure C atoms and each of atoms has four valence electrons, three of them form tight bonding with neighbors in the plane. Their wave function takes the form,

$$\frac{1}{\sqrt{3}}(\psi_e(2s) + \sqrt{2}\psi_e(\tau_i 2p)\ ,\ (i=1,2,3) \qquad (1.1)$$

In equation (1.1), $\psi_e(2s)$ is the (2s) wave function for C, and $\psi_e(\tau_i 2p)$ is the $(2p)$ wave functions of which the axes in the direction τ_i joining the graphite atom to its three neighbors in the plane. The fourth electron is in the $2p_z$ state which gives rise to graphene an extraordinary electrical conductivity [12].

Hexagonal layer of graphene has unit cell consisting of two C atoms in figure (1.2a). The interatomic distance between C atoms in the unit cell is equal to 1.42Å. The lattice vectors of graphene a_1 and a_2 in figure 1.2(a) can be written as,

$$a_1 = \frac{3a}{2}(\hat{x} + \frac{1}{\sqrt{3}}\hat{y}); \quad a_2 = \frac{3a}{2}(\hat{x} - \frac{1}{\sqrt{3}}\hat{y}) \tag{1.2}$$

In hexagonal lattice of graphene the three nearest-neighbors vectors in real space are given by,

$$\delta_1 = \frac{a}{2}(\hat{x} + \sqrt{3}\hat{y}); \quad \delta_2 = \frac{a}{2}(\hat{x} - \sqrt{3}\hat{y}); \quad \delta_3 = -a\hat{x} \tag{1.3}$$

The reciprocal lattice vectors have magnitude $8\pi/3a$, the first brillouin zone is hexagon as illustrated in (1.2b) and the sides are at a distance $4\pi/3a$ from its centre. In K space the density of electron stated is $2A$ where A is the area of the crystal. The zone has one electron per atom; hence the first brillouin zone of graphene has $2N$ electron state while the second brillouin zone is empty [12, 44]. The Dirac points K and K' are located at the corner of the brillouin zone; their vectors are given by,

$$K = \frac{2\pi}{3a}(\hat{x} + \sqrt{3}\hat{y}); \qquad K' = \frac{2\pi}{3a}(\hat{x} - \frac{1}{\sqrt{3}}\hat{y}). \tag{1.4}$$

The reciprocal lattice vectors shown in figure 1.2(b) are given by,

$$b_1 = \frac{2\pi}{3a}(\hat{x} + \sqrt{3}\hat{y}); \qquad b_2 = \frac{2\pi}{3a}(\hat{x} - \frac{1}{\sqrt{3}}\hat{y}). \tag{1.5}$$

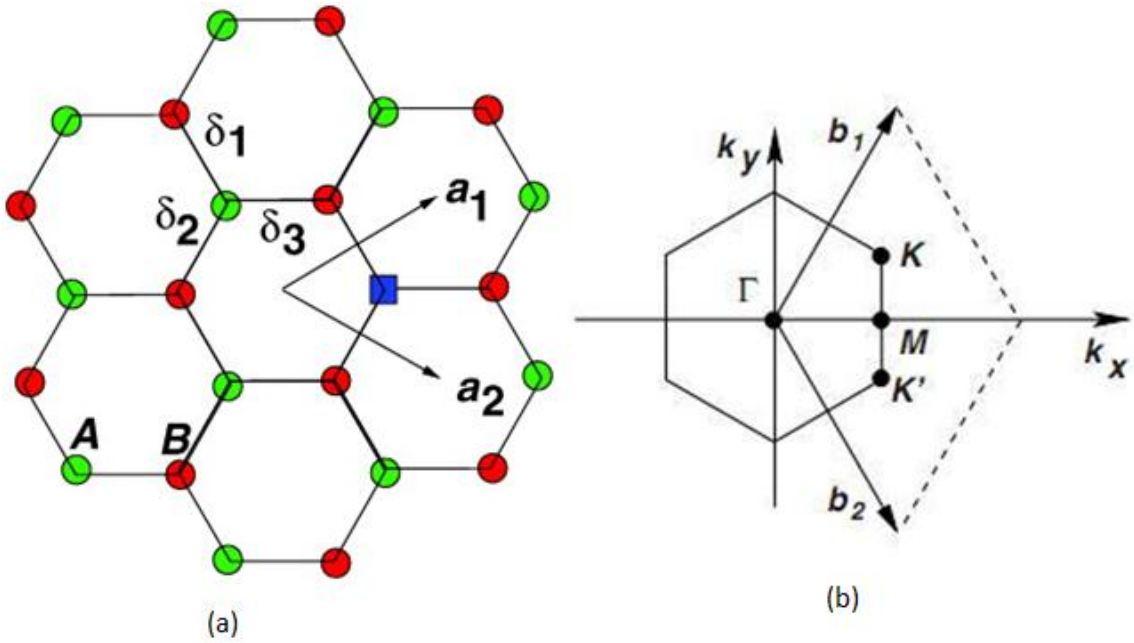

Figure 1.2. The lattice unite vectors $\vec{a}_1$ and $\vec{a}_2$ and the nearest neighbors δ_1, δ_2 and δ_3. *AB* represent the interatomic distance a, (b) the first brillouin zone of the honeycomb lattice and the Dirac points *K* and K' at the corner [12, 44, 45].

Beside the realization of graphene as 2D membrane, atomistic of thin graphene strips addressed primarily to study the nature of edge dislocation and the appearance of defective dangling bonds in carbon networks [13] .Such a graphene strips known as graphene nanoribbons and not expected to be found in nature. Nanoribbons have two types depending on the edge shape, which are armchair graphene nanoribbons and zigzag graphene nanoribbons as shown in figure (1.3). When graphene layers stack on top of each other give graphitic material and multiple stacking give multiplayer graphene nanoribbons [8].

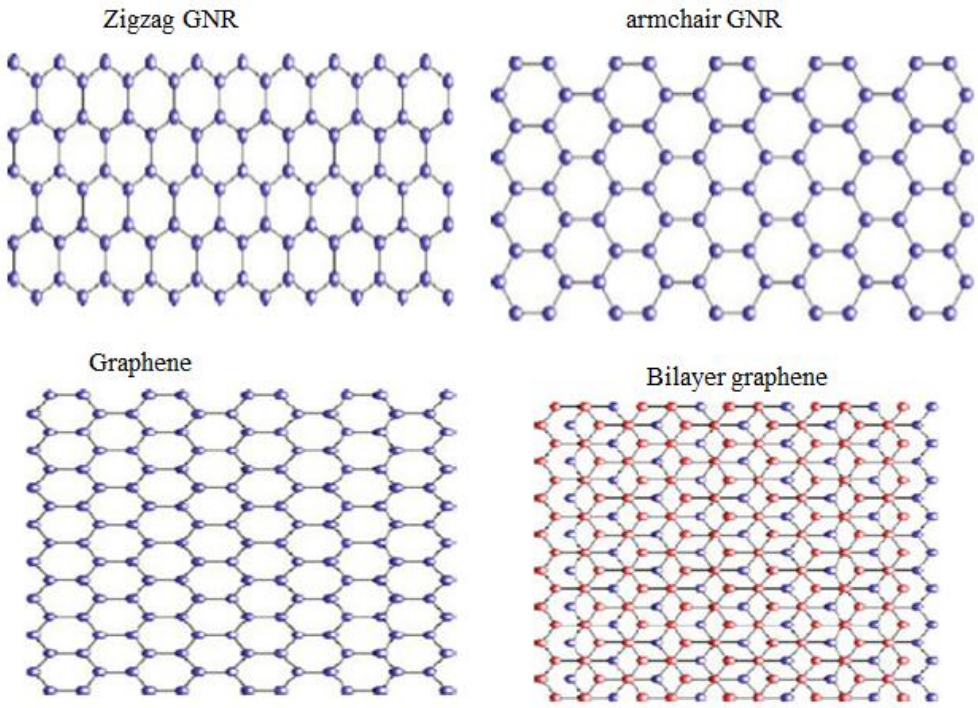

Figure 1.3. Graphene nanoribbons with armchair and zigzag.

CHAPTER 2

GRAPHENE, PHYSICAL PROPERIES AND SYNTHESIS

2.1. Crystal and Electronic Structure of Bulk Graphite

Graphite is lamellar material consisting of stacked layers of graphene as ilustrated in Figure (2.1) [3]. (lamella is a small plate used to refer to collections of fine sheets of a material held adjustment to one another while lamellar structures or known as microstructures are composed of fine layers in the form of lamella).

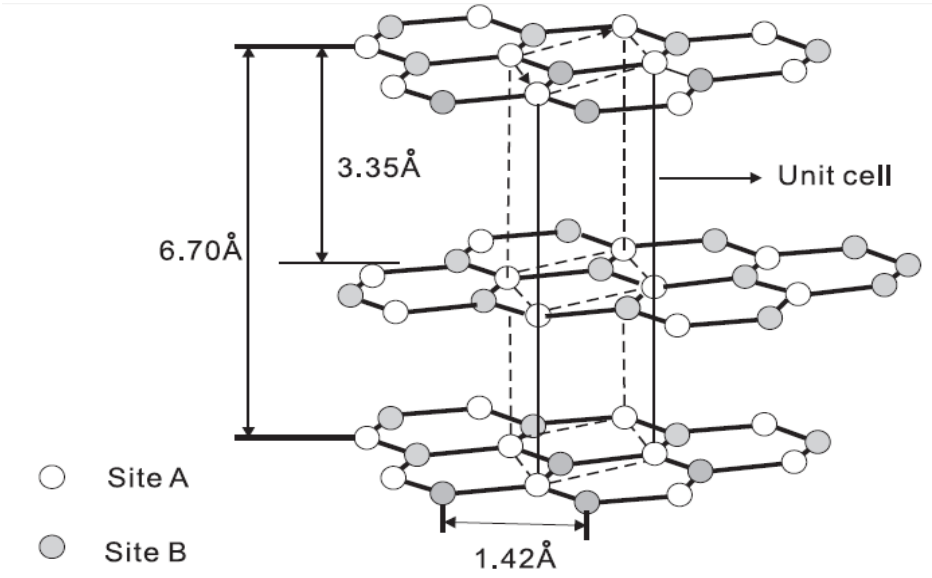

Figure 2.1. Crystal lattice structure of graphite

In graphene C atoms are sp^2 hybridized and covalently bonded in order to form hexagonal two dimensional arrays. In graphene matrix C to C distance is 1.42Å which leads to a lattice constant of about 2.46Å. In graphite the graphene layers are bonded with van der Waals force and the space between the adjacent graphene layers is 3.35Å [3].

Graphene layers stacked in different sequences but the most common is called Bernal graphite (with AB stacking sequences) and rhomobohedral graphite (with ABCBC stacking sequences). In Bernal structure C atoms in layer B are directly located

above the centre of C hexagon in the layer A. In rhomobohedral structure the centres of C hexagon in the A is directly located below the corner of the hexagon in layers B which is turned directly below a non-equivalent corner of hexagon in layer C as shown in figure (2.2)[3].

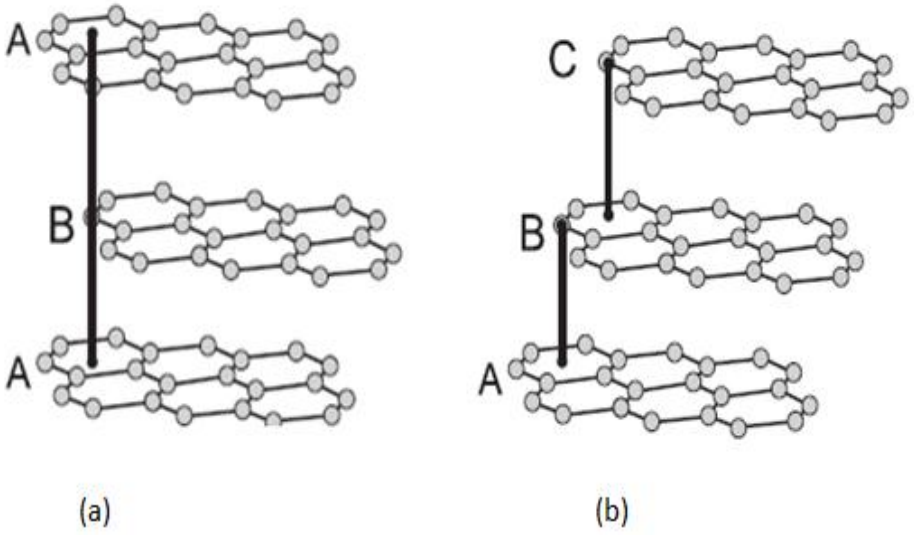

Figure 2.2. (a) Bernal graphite ABAB (b) rhomobohedral graphite.

The Van der Waal's force between the graphene layers is very weak. Therefore the first band structure calculations neglected the interlayer interaction between graphene layers, hence graphene was proposed as an approximation model for graphite. However this weak interlayer interaction caused a significant difference between graphene and graphite, where the band structure of graphene has zero band-gap. Graphite has band overlap and thus graphite shows semi-metallic properties with electrons and holes [3].

Graphite crystal structure has two equivalent atomic sites, A and B as shown Figure (2.1). At site A, C atoms have neighbours directly above and below in adjacent graphene layers while at site B they don't. The unit cell of graphite contains four atoms as illustrated in Figure (2.1). The Brillouin zone of the reciprocal lattice illustrated in Figure (2.3).

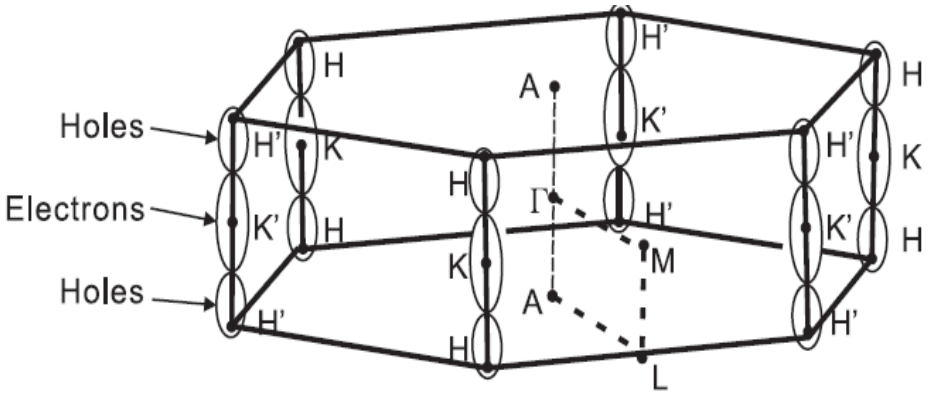

Figure 2.3. Brillouin zone with several high symmetry points electron and Fermi surface are located along the edge of HKH and H′ K′ H′.

The electronic energy bands near HK axis correspond to three Dimensional's graphite as illustrated in Figure (2.4). C atoms have four valence electrons; therefore there are totally 16 bands, 12σ bands and 4 π bands. The energies in the π band are within the 6 antibonding σ bands and 6 bonding σ band. The two π bands are antibonding while the 2 π bands are bonding. Along the Brillouin edges of HKH and H'K'H the four π bands are labelled as E_1, E_2, E_3 (doubly degenerate). E_1 band is empty, E_2 nearly full and defined the minority of the holes near the zone corner, E_3 partially occupied and defined the majority electron and holes pockets [3].

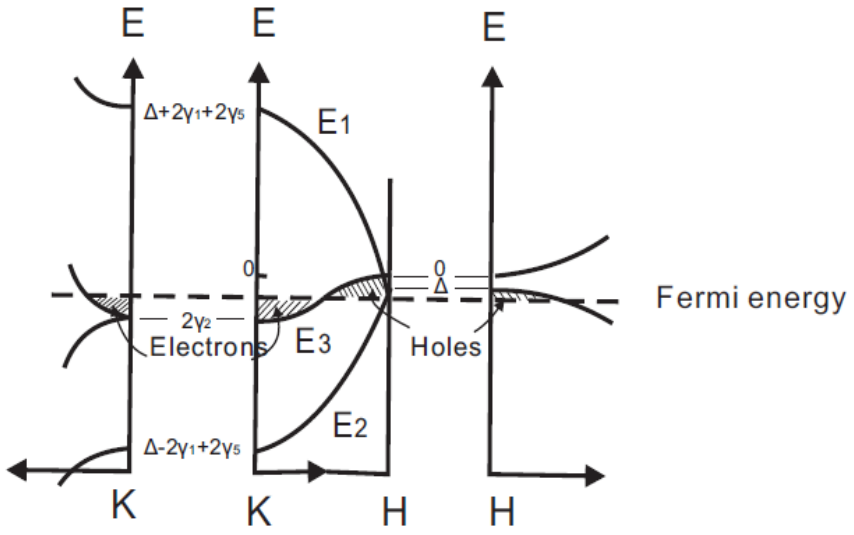

Figure 2.4. Electronic energy bands near the H-K-H axis in the three dimensional graphite. The E_3 band is doubly degenerate along the H-K-H axis (see canter figure) and is lifted when away from the H-K-H axis (see left hand and right hand figures)

The interlayer interaction has strong effect on the four π band near the Brillouin zone edges causing a band overlap of about 40meV. Due to the weak interlayer interaction in graphite, carrier transport is essentially two dimensional. Graphite exhibits large electrical anisotropy with high in-plane conductivity (σ_α approximately 10^4 $\Omega^{-1}cm^{-1}$) and low c-axis conductivity σ_c which approximately 10 Ω^{-1} cm^{-1}. The higher ratio of σ_α to σ_c indicates higher graphite quality. Besides graphite has high in-plane mobility of approximately $10^4 cm^2/Vs$ at room temperature and approximately 10^5-10^6 cm^2/Vs at 4 K. Due to electron-hole restitution near Fermi level, graphite has low free carrier concentration of about 10^{-4} per atom at room temperature [3]. In general, graphite shows complicated transport properties concerning carrier density, mobility, conductivity and anisotropy, which are temperature dependent.

2.2. Crystal Structure and Physical Properties of Graphene

Physics of graphene became very interesting since the experiment realization of mono-crystalline graphene. Its unique band structure equivalent to relativistic massless particle gives rise to unusual electronic properties to graphene. Monolayer graphene consists of carbon atoms arranged in two dimension honeycomb crystal structure. Honeycomb lattice of graphene shown in figure (2.5), consists of two interpenetrating triangular sub-lattice. The site of one sub-lattice (green) is the centre of triangles defined by other site (orange one) as illustrated in figure (2.5) [5]. The lattice consists two C atoms per unit cell and is invariant under 120^o rotational around any lattice site. Each atom has one ***s*** and three p_{xy} orbitals. The ***s*** orbitals and two in-plane ***p*** orbitals are tied up in graphene's strong covalent bonding and do not contribute in its conductivity and the remaining p_z orbitals oriented perpendicular to the molecular plane [5].

The initial theoretical efforts to study graphene's 2D electronic structure was made by P.R.Wallace in 1947 followed by its extension to the electronic structure of 3D graphite by D.F.johnston. J.W.McClure and M.Yamazaki. McClure also emphasized that the quasiparticle were Dirac-like which was re-iterated by G.Semenoff [8]. The studies showed that, graphene is a semi-metal which shows zero bandgap with linear dispersion around the chemical potential this leads the cones in two dimensional reciprocal space; it was quite surprising that most of the matter waves have quadratic dispersion and following Schrödinger equation which is first order in space and time.

This leads to the following dispersion for the conduction and valance band respectively [8].

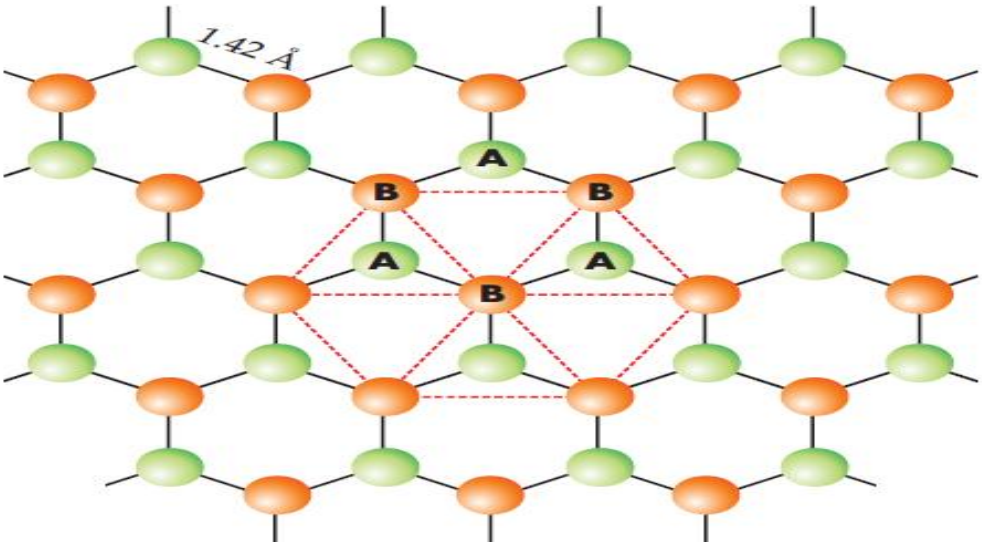

Figure 2.5. Honeycomb lattice of graphene consists of two interpenetrating triangular sub-lattice. The site of one sub-lattice (green) are at the centre of triangular defined by the other (orange).The lattice has two C atom, A and B per unite cell and is invariant under 120^{o} rotational around any lattice site [5].

$$E_s(k)=E_{c.v}+\hbar^2|k|^2/2m_{c.v} \qquad (2.1)$$

$E_{c,v}$ is the conduction and valence band edges and m_c and m_v are the effective masses of electrons in conduction band and holes in the valance band, respectively (m_v is negative). For $E_C=E_v$ the dispersion still remains quadratic. In contrast to Schrödinger equation the dispersion for the Dirac equation is,

$$E_D(K) = \sqrt{m^2c^4 + \hbar^2c^2|K^2|} \qquad (2.2)$$

Where c, is the speed of light, m is the relativistic mass (D Ξ Dirac) [8]. Positive and negative dispersion plots are illustrated in figure.1.8, which give rise to mass dependent gap of $2mc^2$ between the positive energy of matter (electron in this case) and the negative energy of anti-matter (positron)-The product mc^2 for an electron is about 0.512MeV but in the limiting case of m=0 leads to zero bandgap thus the equation (2.2) takes the form,

$$E = \pm \hbar c|k| \tag{2.3}$$

Which is also plotted in figure (2.6).The figure depicts the linear dispersion with zero bandgap, the energy scale is on the order of MeV with the speed is equal to the speed of light (c) [8].

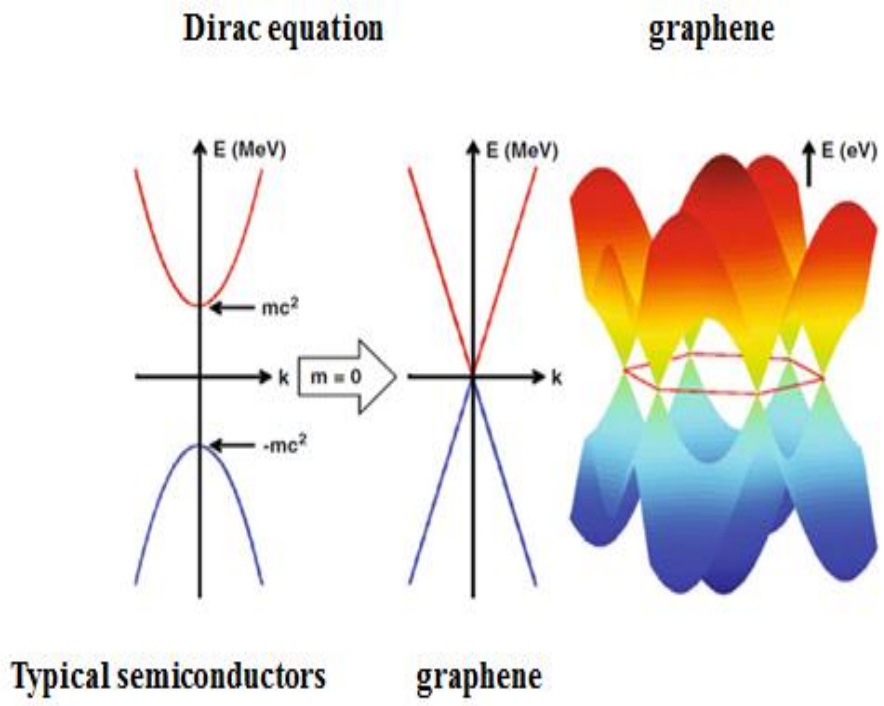

Figure 2.6. Graphene band structure Dirac dispersion with $2mc^2$ gap are shown when m=0 the gap become zero, in the same way graphene band structure has linear dispersion with zero band gap around the Dirac point with energy in eV [8].

Graphene band structure shown in the figure (2.6.) can be produced by the equation (2.4) based on the tight-binding description [2]

$$E_G(k) = \pm t\sqrt{1 + 4\cos\left(\frac{3k_x\, a_{cc}}{2}\right)\cos\left(\frac{\sqrt{3}k_y\, a_{cc}}{2}\right) + 4\cos^2\left(\frac{\sqrt{3}k_y\, a_{cc}}{2}\right)} \tag{2.4}$$

where a_{c-c} = 1.42Å is C-C bond length and t is first nearst neighbour tight binding parameter(G Ξ Graphene). It is clear that the bandgap is zero and dispersion is

linear around the point where the conduction and the valence band meet with renormalized velocity ν resulting in,

$$E_{G=} \pm \hbar\nu|k| \tag{2.5}$$

Similar to the despersion of Diracs particles in equation (2.3) this suggests that electrons and holes behave like Dirac fermions in graphene with zero mass and zero bandgap. This means that the charge carriers in graphene behave like massless relativistic Dirac fermions with point of intersection between conduction and valnce bands which is called Dirac point. Moreover, there are six points over the Brillioun zone where the conduction and valence band meet as illustrated in figure (2.6) [8]. Equation (2.1) for ordinary metal and semiconductor while the equation (2.5) for graphene. In equation (2.5), ν corresponds to fermi velocity of the elctron in graphene. Furthermore equation (2.5) implies that the speed of electron in graphene is constant and independent of momentum like photons [4]. Recently it was found that the speed of electron in graphene is about $10^6 ms^{-1}$,which is large but still slower than the speed of light in vacuum. because the electron are sluggish compared to the speedy photons, they exchange when interacting, the physics of electron-electron interaction in graphene is different from the physics of photon mediate interaction between fermions in quantum electrodynamic (QED). In graphene the interaction among electron are extremly strong and graphene dimensionless coupling constant($\alpha_{GR}=e^2/\hbar\nu_f \approx 1$) is much larger than that of of QED $\alpha=\frac{e^2}{\hbar c} \approx 1/137$. Here the large diferent between c and ν, implies that the interacting electrons in graphene sheets is not like the 2D version of QED [4, 47].

2.3. Graphene Synthesis

The earlier works focused on how to get graphene from graphite using different methods such as chemical exfoliation and intercalation graphite, so that graphene planes separated by layers of intervening atoms or molecules [2]. Recently a single and few layer graphene have been grown by chemical vapour deposition (CVD) of hydrocarbons on metal (substrate) and thermal decomposition of SiC in vacuum or inert gas environment [2].The films are usually studied by surface measurements techniques including and scanning probe microscope techniques such as AFM and STM.

2.3.1. Graphite Intercalation Compound

Graphite intercalation compounds generally form by inserting atomic or molecular layers of a different chemical species between layers in a graphite host material as shown in figure (2.7) [15]. The inserting molecule known as guest. These materials have the formula (XC_y), where the ion X^{n+} or X^{n-} is intercalated atoms or molecules between the graphite layers ($y < 1$). When graphite and the guest X interact by charge transfer, the in–plane electrical conductivity generally increased. When the inserted molecules form covalent bound with graphite layers as in fluoride or oxide, the graphite conductivity decrease as it conjugate sp^2 collapses. In general the interaction is revisable and takes the form: $C+YX \rightarrow CX_Y$ [16, 26, 27].

One of the famous GICs is KC_8 prepared by melting potassium over graphite powder. The potassium is absorbed into the graphite and the material changes the colour form black to bronze as illustrated in figure (2.8). The potassium to potassium distance is assumed to be twice the distance between the hexagons in the carbon framework in order to explain the composition. The anionic graphite layers and potassium cations bonded as ionic bond and the electrical conductivity of the materials is greater than the α bond in the graphite(*α-cleavage in organic chemistry is refer to the act of breaking Carbon to carbon bond adjacent to Carbon bearing a specified functional groups: α-cleavage (alpha-cleavage)". IUPAC Compendium of Chemical Terminology (Gold Book)*), and since the KC_8 is superconductor ($T_{critical} = 0.14$ K) then heating KC_8 leads to the formation of series of decomposition products as the potassium atoms are eliminated as shown in the process: $3\ KC_8 \rightarrow KC_{24} + 2$ K.[16].

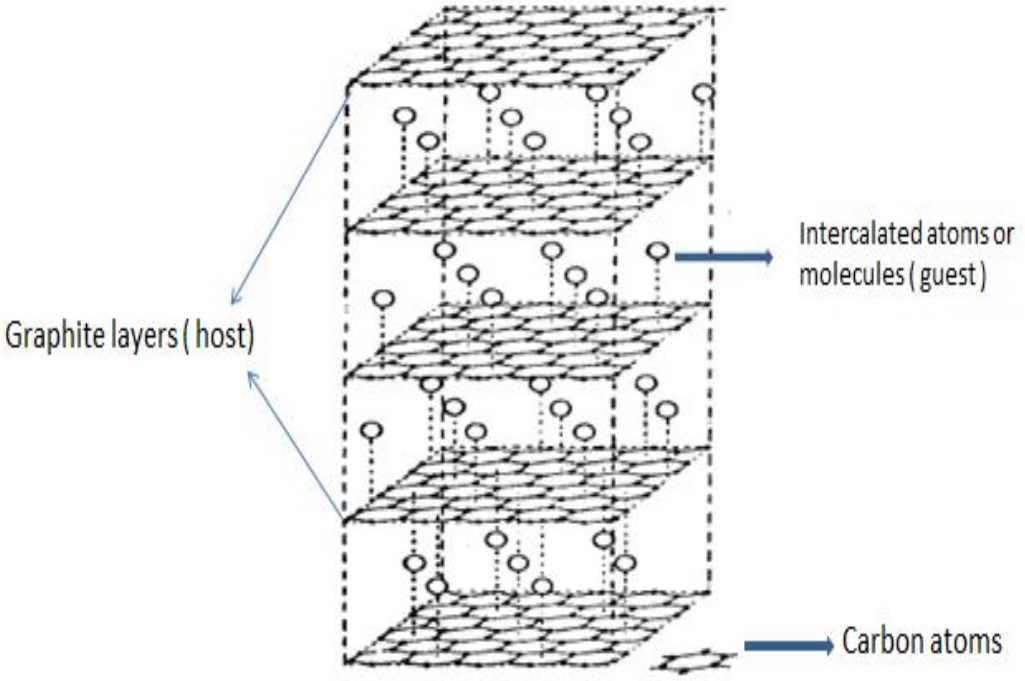

Figure 2.7. Intercalated atoms or molecules (guest) in between graphite layers (host) [15].

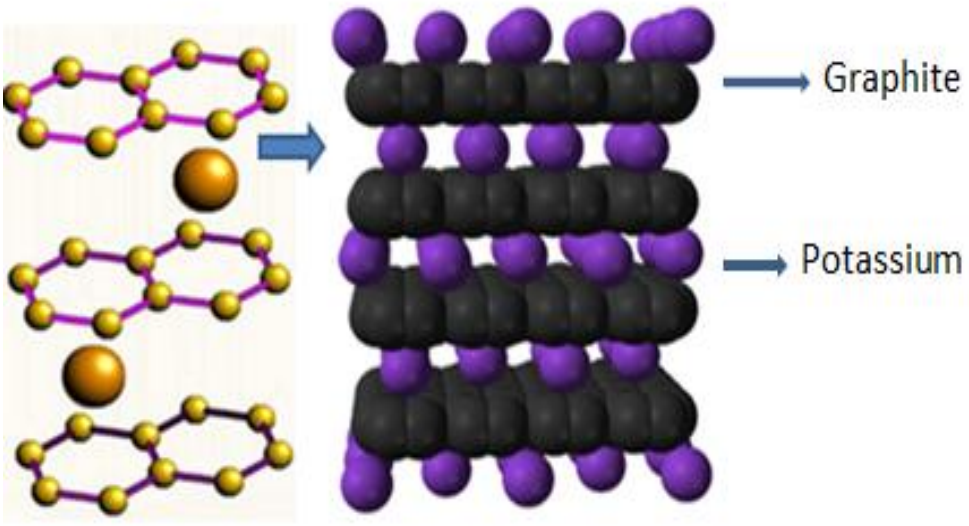

Figure 2.8. GICs, KC_8 prepared by melting potassium on graphite powder [27, 28].

2.3.2. Micromechanical Cleavage Method

Micromechanical cleavage method based on using bulk graphite and exfoliates into individual planes .In the recent methods; growth of graphene requires very high temperature while the exfoliation method can be done at room temperature. The process is similar to process when we write using a pencil, because during writing we separate the graphite layers, but exfoliation technique involves many carefully steps than writing with pencil, and then thin graphitic films obtained. But even for 20 layers, thick graphite generally behaves like bulk graphite. The real breakthrough came when monolayer of graphene obtained in 2004 by using technique known as micromechanical cleavage. In this method, the top layer of high quality of graphite crystal removed by a piece of adhesive tapes, with graphitic crystallites and then pressed against the substrate of choice like SiO_2. If the adhesion of the bottom graphene layer to substrate is stronger than that between graphene layers, graphene layers can be transferred onto the surface of substrate. This simple method produces extremely high quality graphene crystallites. In principle, this technique works well with practically any surface which has reasonably high adhesion to graphene. In the earlier experiments using this method (as it is done by Novoselov and Andre Geim in Manchester University), the process was extremely low. In order to find micrometre-sized graphene flake, macroscopically large area need to be scanned. And is it all seems to be difficult especially Atomic Force Microscopy AFM used. Because, the area that needs to be scanned is in nanometre scale. In this case, optical microscope have to be used and monolayer of graphite on some substrates (Si/SiO_2 with 300 nm SiO_2 layer) can produce an optical contrast up to 15% for some wavelengths of incoming light. The first characterization by optical microscope for the graphene produced by using micromechanical cleavage shown in figure (2.9) [13].

We also grew graphene by micromechanical cleavage in our laboratory (Nano-physics research group at Izmir Institute of Technology). We performed Raman measurements in different areas to see multilayers and monolayers as shown in figure (2.10).

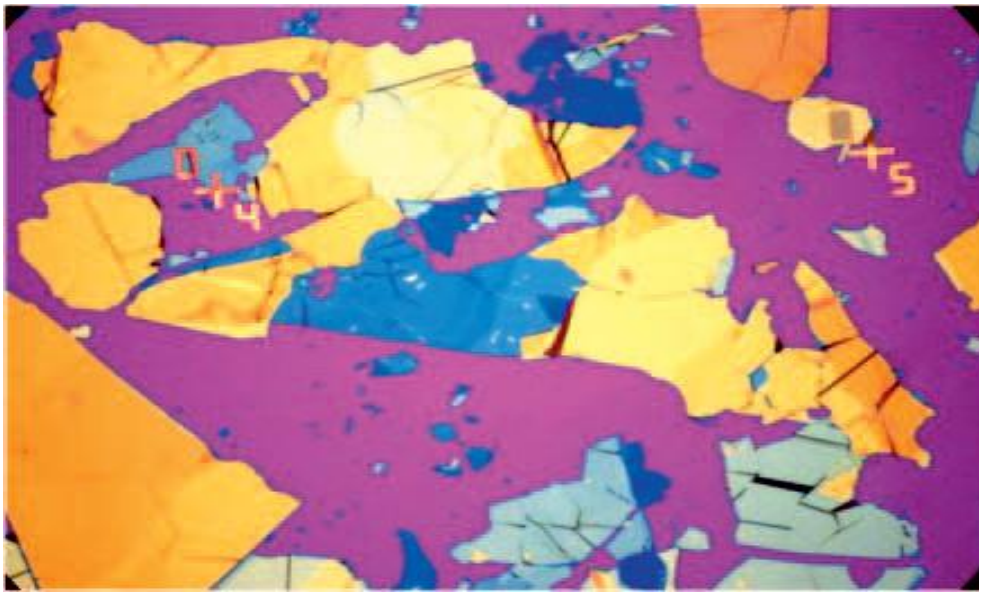

Figure 2.9. The graphitic flake on surface of Si/SiO_2 wafer (300 nm of SiO_2 purple colour) the different colour correspond to the flake of different thicknesses ~ 100 nm (the pale yellow one) to few manometers (a few graphene layers of most purple ones). The scale is given by the distance between lithography marks 200μm [13].

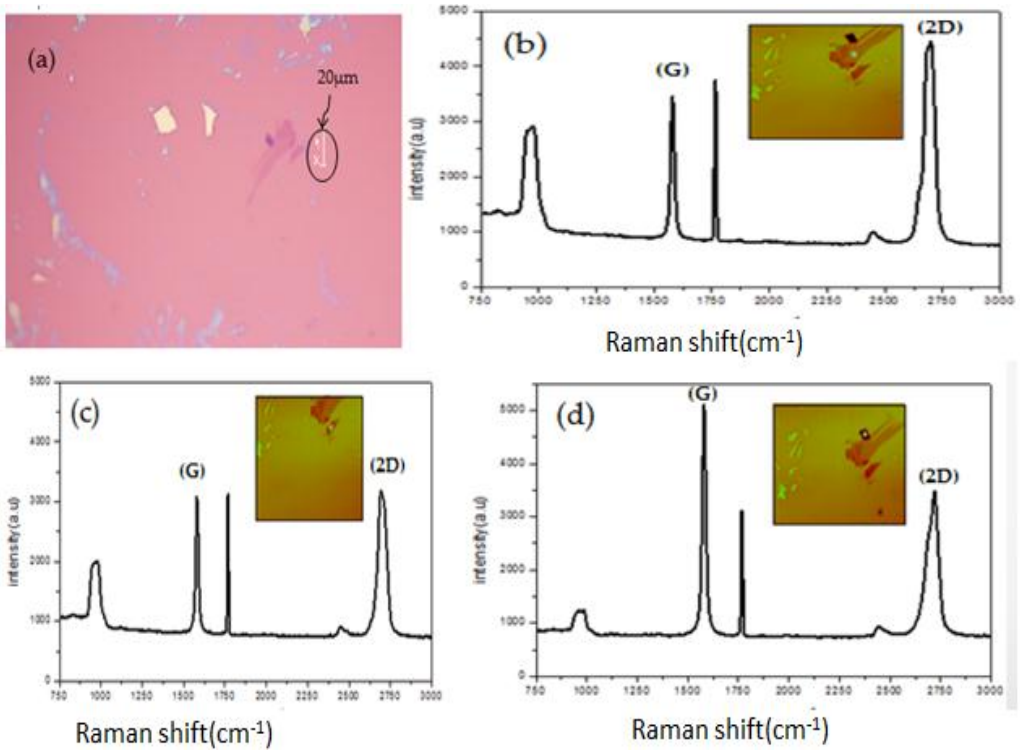

Figure 2.10. (a) graphene layers grown by micromechanical cleavage (b) Raman measurement in an area contains multilayers according to 2D peak (c) and (d) showing 2D peak with intensity lower that happening in(b) indicating few layers graphene

2.3.3. Chemical Vapour Deposition (CVD) Growth of Graphene

CVD is a chemical technique that is used to produce large scale thin solid film (material) by deposit the film on substrate from the vapour species through chemical reaction. CVD based on the chemical reaction and that makes it a suitable technique which distinct compared to other techniques such as physical vapour deposition (PVD). During the CVD process, the gas feds into the reactor by a gas delivery system, which must consist necessary valve, gases flow manipulate by mass flow controller (MFCs). The gas mixing unit is responsible for mixing gases before let into the reactor where the chemical reaction used to deposit the materials. The reactor is surrounded by heater to provide high temperature for the reaction. Then the by-product of the reactions and non-reacted gases removed by the gas delivery system. The schematic of typical tube furnace CVD illustrated in Figure (2.11) [6].

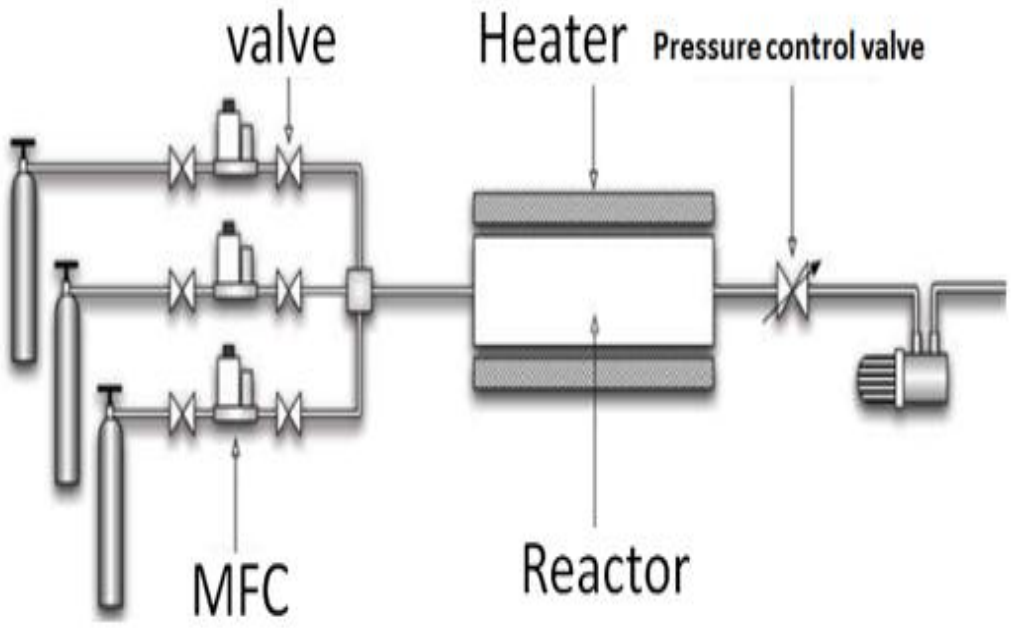

Figure 2.11. Schematic of typical tube furnace CVD .The gas flows are regulated by mass flow controller (MFCS) and Fed into the reaction through gas distribution unit and chemical deposition take place in the reactor that is heated by the outside heaters. The exhausted gases are removed by the vacuum pump [6].

CVD starts by diffusing the reactance through the boundary layer, then adsorb onto the substrate surface where the chemical reaction is occurs. After the chemical reaction is done, the by-products desorb form the surface, then the by-products diffuse through the boundary layer as shown in figure (2.12) [6].

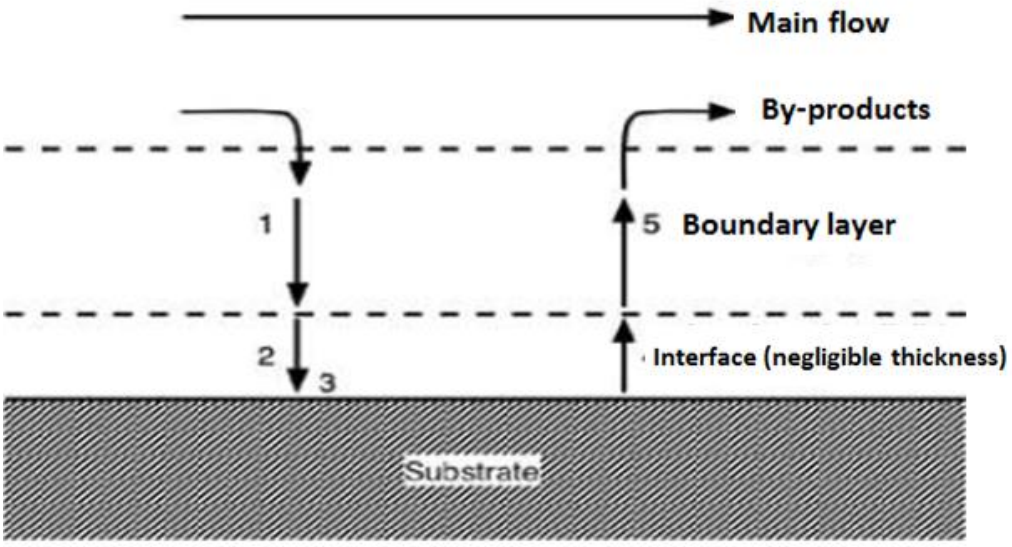

Figure 2.12. 1-Reactance diffuse through the boundary layer 2- reactance are adsorbed onto substrate surface 3- chemical reaction occurs on the surface 4-the by-product of the reaction are desorbed from the surface 5- the by-product diffuse through the boundary layer [6].

During the growth process of carbon nanotube (CNT), active metals called catalysts have non-filled d-shells such as Fe, Ni and Co; have been used as synthesis of CNT through CVD. These metals commonly have relatively high C solubility which makes adsorption and interaction with hydrocarbons easier. The same idea can be used to grow graphene and the quality of the graphene grown layers depend on the ability of transition metal (catalyst) to interact with incoming hydrocarbon (generally CH_4) [7]. The formation of graphene on transition metals through CVD follows two steps, One called as the dissolution in which C atoms incorporate into the metal and the other one called as segregation (formation of graphene through rapid cooling) [7]. The first successful graphene deposition by CVD method, is done by Ni as catalyst [6]. The sample is prepared and is loaded into the furnace, then the whole reaction chamber pumped down to base pressure of P = 1.0×10^{-5} mbar (low pressure CVD), then hydrogen gas is sent into the reaction chamber and the furnace is turn of up to the

deposition pressure the temperature maintained for some time so as to anneal the catalysts. To initiate grain growth deposition process starts by letting CH_4 together with H_2. Finally the whole chamber cooled down before taking the sample out [6].CVD graphene growth illustrated in figure (2.13).

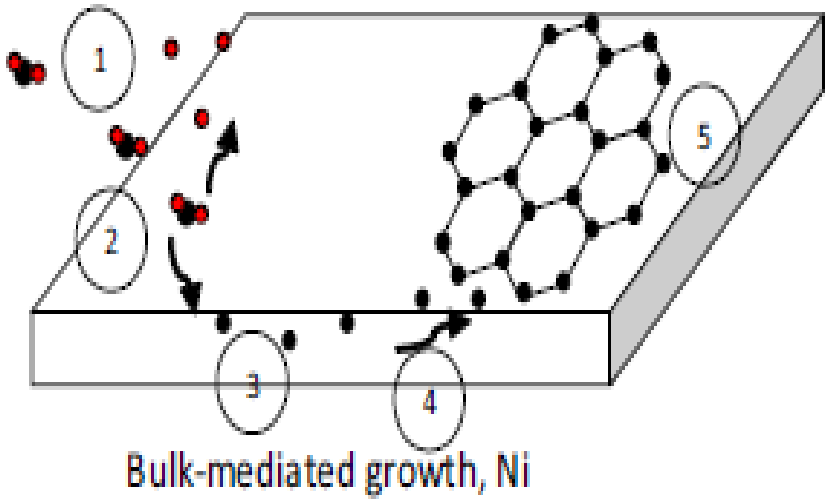

Figure 2.13. 1-Hydrocarbon chemisorbs on the metal. 2-hydrocarbon dissociate through dehydrogenation. 3- Dissolute carbon atoms diffused into the bulk metal (catalysts with empty d-shells). 4- Excess carbon atoms diffuse to the surface, before step number 4 segregation process starts when the concentration of carbon atoms in the bulk has achieved the threshold for nucleation or during the cooling process 5-segregation does not stop until the concentration in the bulk reach the equilibrium [7].

In order to avoid diffusing of the metal atoms into the substrate, SiO_2 placed in the inter-face between metal and substrate as shown in figure (2.14).

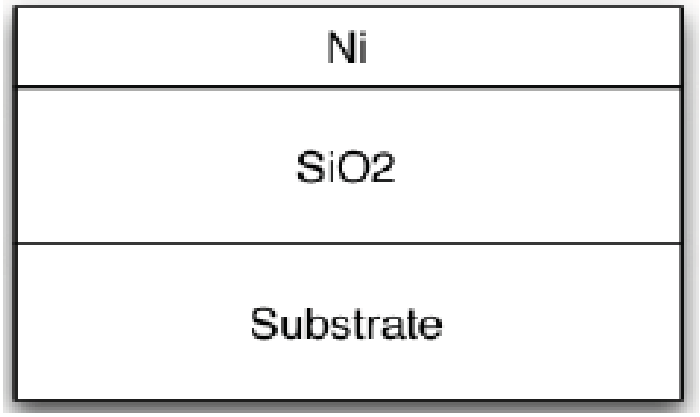

Figure 2.14. SiO_2 placed between metal and substrate to prevent metal atoms to not diffuse into the substrate.

Although CVD is a promising technique it has disadvantages especially when we speak about how to control the process. Because controlling the regular parameters (i.e. temperature, pressure and time), there are other factors which might affect the growth process in CVD method. For example chemical reaction might be complicated because the reaction usually involves many intermediate steps and no one can know the exact step by step reaction mechanism. One must consider the depletion of the reactance from one end of the reactor to another end [6], and all the factors in CVD are connected to each other. Hence, CVD is a complex process and it's necessary that many tests should be performed before a successful deposition of thin film that is required.

CHAPTER 3

EPITAXIAL GRAPHENE

The successful development in garphene-based electronic devises depends on the large scale production of the graphene material. Several methods for graphene production have been proposed [20]. The commonly used method to produce graphene are by repeatedly cleaving thin graphite layers by using so-called scotch tape method (Mechanical exfoliation).The graphene layers that produced via mechanical exfoliation are randomly distributed flakes and size restriction on a wafer making it unsuitable for industry applications and it requires transfer to an insulating substrate, with the methods that have yet to be developed. Another production method called as Chemical vapour deposition (CVD) on a metal substrate. Although this method is a recent method, it can be very complicated and controlling the chemical reactions seems to be difficult.

The preparation of a single layer or few layers graphene grown epitaxially by the thermal decomposition of SiC has been proposed as a viable route for the synthesis of uniform, wafer-size graphene layers for technological applications [20]. Epitaxial graphene is compatible with existing Si-based technology; a considerable advantage of this method is that insulating SiC substrate can be used so that transfer to another insulator is not required. However the large-scale structure quality is limited by the lack of continuity and uniformity of the grown film [20].

3.1. What Is Epitaxial Graphene

Epitaxial graphene is one layer of graphene grown epitaxially on a substrate; it reveals different properties depending on the substrate on which it is grown [17].

Si has been the material of choice for electronic devices since many decades. However, in the near future, fundamental property limitations of Si will inhibit the ability to fabricate operational devices and circuits due to continuing device size reduction. The ability to reduce device size and thus pack more and more devices on a chip has allowed adherence to Moore’s Law.

Epitaxial graphene has extraordinary electronic properties that offer the possibility of greatly enhanced speed and performance relative to silicon; this material is expected to serve as the successor to silicon in integrated circuits and microelectronic devices .

3.2. SiC and Its Polar Surfaces

Before discussing the growth of epitaxial graphene on SiC in ultra-high vacuum chamber here is brief discussion about SiC and its polar surfaces.

SiC can be produced in much different crystalline modifications (more than 200 type), called polytypes [8, 31]. These polytypes have basic building blocks as shown in figure 3.1. Due to the sp^3 hybridization of the Si and C atoms s and p valence orbitals, Si and C atoms are bounded to four neighbors in tetrahedral arrangement Figure 3.2 where the bounds are characterized by significant degree of iconicity due to the different electronegativities of the two elements which are 1.9(Si) and 2.55(C) [8, 29, 30]. Bilayers consisting of the edge connected Si-C tetrahedral are formed from the individual tetrahedral as shown in figure (3.2b) [8].

Bulk crystal of SiC is formed by stacking bilayers on top of each other which has two different stacking arrangement, cubic stacking (e.g. 3C-SiC) and hexagonal stacking(e.g. 4H-SiC and 6H-SiC) are possible which are shown in fig3.2(c). Cubic stacking corresponds to cubic zinc blende structure and hexagonal stacking is found in hexagonal Wurzite structure. According to Ramsdell notation these structure are referred to as 3C structure and 2H, 4H, 6H…etc. referred to hexagonal structure respectively [Ramsdell notation is the notation that specifies the total number of the layers contained in a possibly (large hexagonal) unit cell and then add the letters H, C, OR, R to denote the overall lattice type as being hexagonal cubic or rhomobohedral respectively.]. As shown in figure (3.1), these two different stacking arrangements are mixed in periodic form to create more than 200 known polytypes. Two of these polytypes are hexagonal polytypes 4H-SiC and 6H-SiC as shown in figure (3.2). In these two polytypes the unit cells contain 4 and 6 bilayers respectively. All SiC polytypes are semiconductors with band gap varies from 2.39 eV for 3C-SiC over 3.02eV for6H-SiC to 3.27eV for 4H-SiC [8, 32]. Intrinsic or compensated SiC is insulating. This is great advantage of SiC to be used as a substrate for graphene growth.

The later (4H-SiC) can be directly patterned into device without prior transfer to another substrate, which is case for graphene grown on metals [33]. Both 6H-and4H-SiC structures can be used for growing epitaxial graphene, because commercially became available as substrates. Both the (0001) and (000-1) polar surfaces of 4H-SiC and 6H-SiC have hexagonal crystal geometry, it become compatible to grow graphene. Here (0001) and (000-1) surfaces correspond to the Si-face and C-face respectively [8].

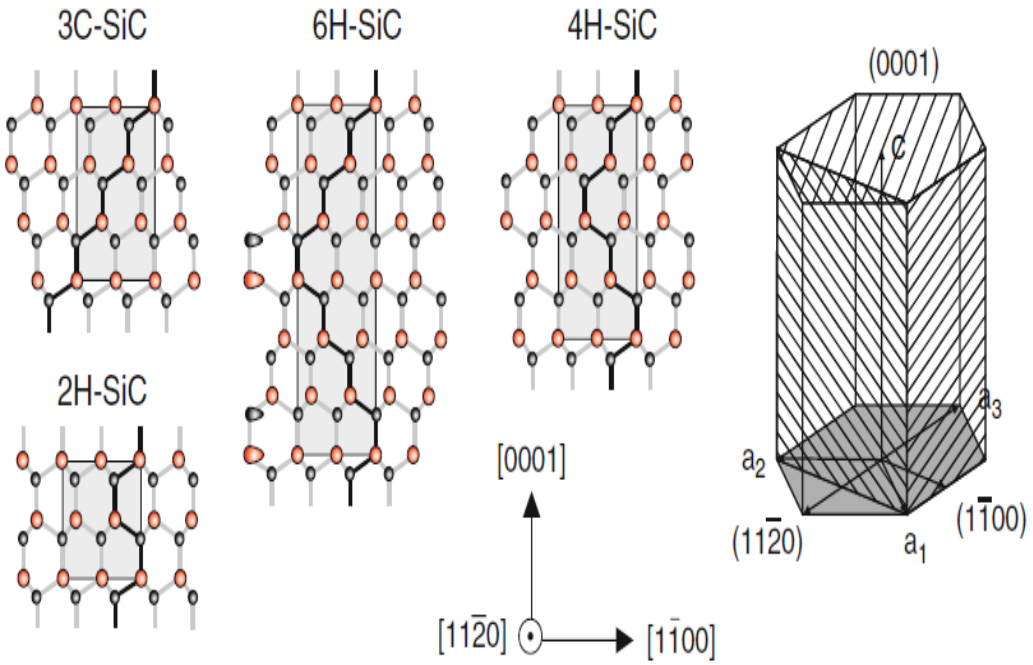

Figure 3.1. Four different polytypes of SiC, in the hexagonal structure of SiC unit cell indicates the orientation of the (0001), (11-20) and (1-100). The surface has only Si atoms in the topmost layers and the opposite face only C atoms. The latter is called (000-1) surface [8].

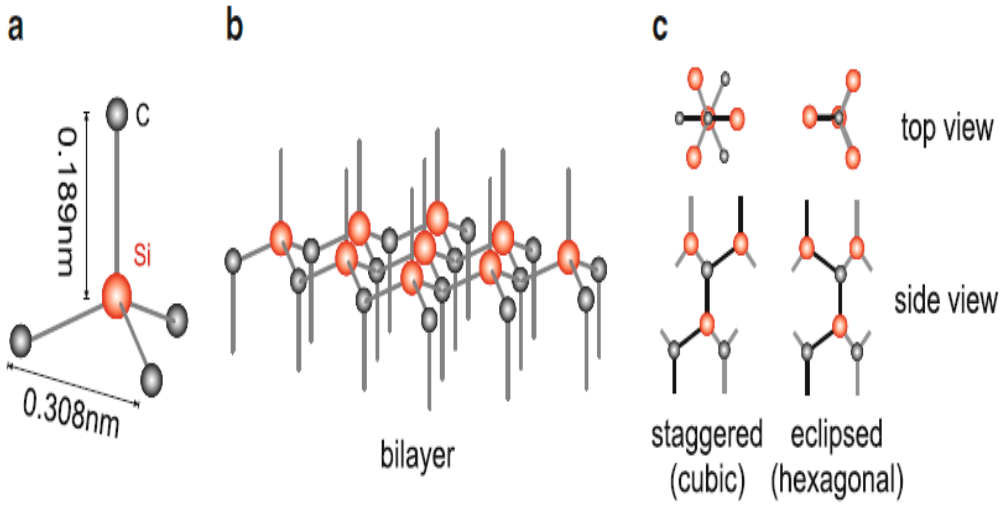

Figure 3.2. Structure elements of SiC (basic building blocks). (a)Tetrahedral bonding arrangement; (b) bilayer. (c) Two different stacking arrangements [8].

3.3. Growth of Epitaxial Graphene on SiC In Ultra-High Vacuum

Growing graphene on SiC is in principle relatively a simple task. At high enough temperatures (approximately 1500 ˚C), SiC decomposed into Si atoms and C atoms. Si atoms selectively sublimate from the surface because the evaporation temperature of Si is around 1400 ˚C while that of C is around 3650^{o}C. The carbon atoms however remain at the surface, and the surface converts to rich carbon atom surface and then form stable C-C bond in the form of graphite on SiC. The Phenomenon of creating graphite in this manner known as graphitization of SiC surface. It was first observed by Edward G. Acheson, who has invented the so-called Acheson process to produce SiC (then called carborundum) [8]. Graphitization phenomenon did not gain a lot of interest at that time, but after that the interest on it raised when Berger .et.al showed that this thin graphite exhibit 2D electron gas behaviour.

After that and as earlier as 1975 van Bommel and co-workers found that heating of SiC in ultra-high vacuum leads to evaporation of Si atoms which leave behind carbon rich surface and the excess of C atoms on the surface lead to form sp^2 bond C network . Later it has been shown that these carbon layers orders in a graphite structure, if the formation is finally controlled, graphene is formed rather than carbon nanotubes or carbon nanowalls. This instance together with the fact that SiC is well known wide gap semiconductors (E_{gap} = 3.2ev for 4H-SiC) has led to the majority of research about

epitaxial graphene being focused on SiC as substrate [8]. Recently graphene grown epitaxially on SiC in ultra-high vacuum and many studies have been and are still carried out on layers grown in ultra-high vacuum .The growth process is done by annealing the SiC substrate higher than the evaporation temperature of Si atoms. Ultra High Vacuum (UHV) growth procedures and related phase diagram as shown schematically in figure (3.3) [24]. The sample is normally contaminated by Oxygen and hydrocarbons from the air. After degassing procedure, the sample is annealed inside a UHV chamber. Annealing can be done by e-beam heating process or resistive heating process.

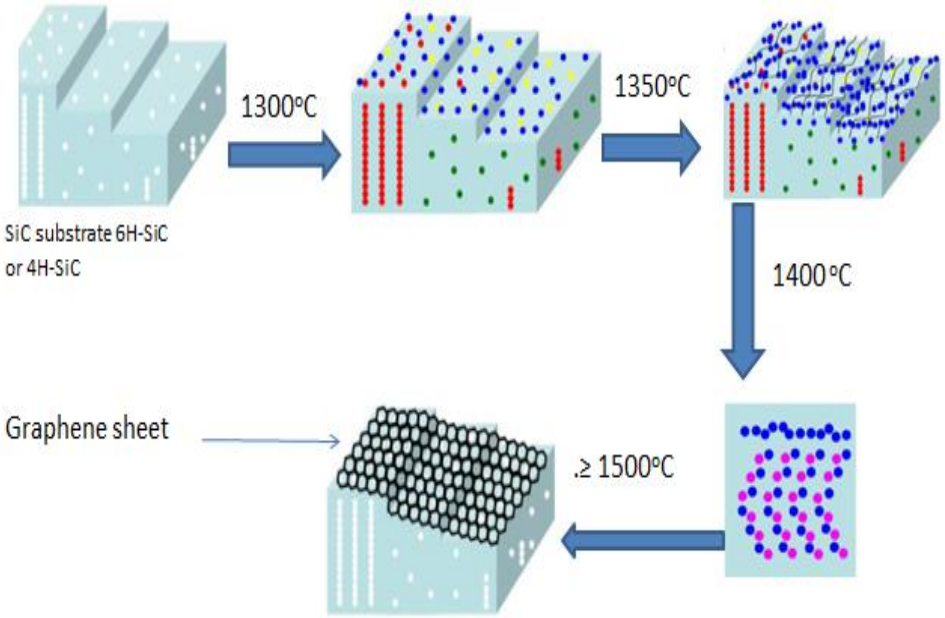

Figure 3.3. Face diagram of UHV growth procedures .Yellow, Red, and Green points, represent Surface defect, Colon defect, and Volume defect respectively. Blue and Purple points represent C atoms and Si atoms respectively [24].

3.3.1. The Mechanism of Graphene Formation

Heating SiC above a temperature of 1400 ˚C, SiC decomposes into Silicon and Carbon. Si atoms sublimate from the surface due to their high vapour density then carbon rich a$(6\sqrt{3}x6\sqrt{3})R30°$ reconstruction evolves. These Carbon layers arrange in a honeycomb lattice to form graphene. One third of C atoms in this reconstruction layers, has covalent bonds to underlying Si atoms of the topmost layers SiC. The reconstructed layers show some graphitic properties and structure but strongly interact with the

substrate, and this leads to electronic properties which is different from isolated graphene. For example the lack of π-bands at the Fermi level and the presence of the band gap.In order to obtain graphene, the annealing temperature must be increased above 1400 ˚C, which leads to new graphene layers formed under already existing reconstruction layers. If Si atoms below the reconstructed layer evaporate, then the covalent bond to the substrate is cut. This bond becomes unstable and cannot connect to any other atoms which force carbon atom to re-hybridizes into sp^2 configuration and develop the typical graphene like delocalized π-bands with neighboring carbon atoms. The evaporated Si atoms leave behind three dangling bonds of carbon atoms in the topmost layers of the substrate. These connect to each other to form interface layers of covalently bound graphene whose structure is the same or identical like reconstructed layers. The layers have evolved into a graphene and interact with interface via Van der Waal's force and then graphene properties can be observed. The next graphene layer formation follows the same manner but this time with converting the interface layer into a graphene layer and the topmost substrate into a new interface layer. The grown new layer under the first layer exhibits a good rotational order of graphene on the C-face surface (0001) of former covalent bonds to the substrate caused rotational fixed position. In contrast, no reconstruction layer is formed on SiC (000-1) due to the differences in surface polarity and as well as the properties of the dangling bonds. This leads to a weak interaction of graphene with the substrate and different growth mechanism which can be explained by the observed azimuthal disorder [9,40, 41,42,43].

3.3.2. Epitaxial Graphene On SiC: Comparison between Si-face And C-face

As it was mentioned in part 3.3.1, SiC has two typical orientations of surfaces, Si-rich (0001) face which is terminated by Si atoms and the other one is C-rich (000-1) face which is terminated by C atoms [34,8,35] a shown Figure (3.4)

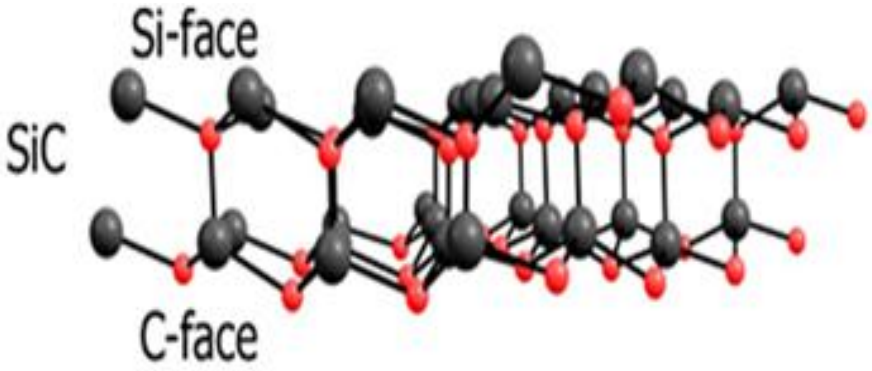

Figure 3.4. SiC faces, Si-terminated face (0001) and C-terminated face (000-1)

On the Si-face SiC graphene layers are stacked in AB Bernal fashion similar to HOPG. However on C-face SiC the layers are rotationally disordered and the stacking sequence shows that graphene layers exhibit an ABC-type stacking. For the same growth parameters (time and temperature), multilayer graphene formed on C-face compared to Si-face [20]. That means the growth rate on the C-face faster than on the Si-face to as illustrated in figure (3.6a) [20]. To show the between graphene grown on C-face and Si-face we performed Raman measurements on both C-face and Si-face, the a sample annealed to 1500 ˚C for about 5 minutes and the results of measurements shown in the Figure (3.5b)

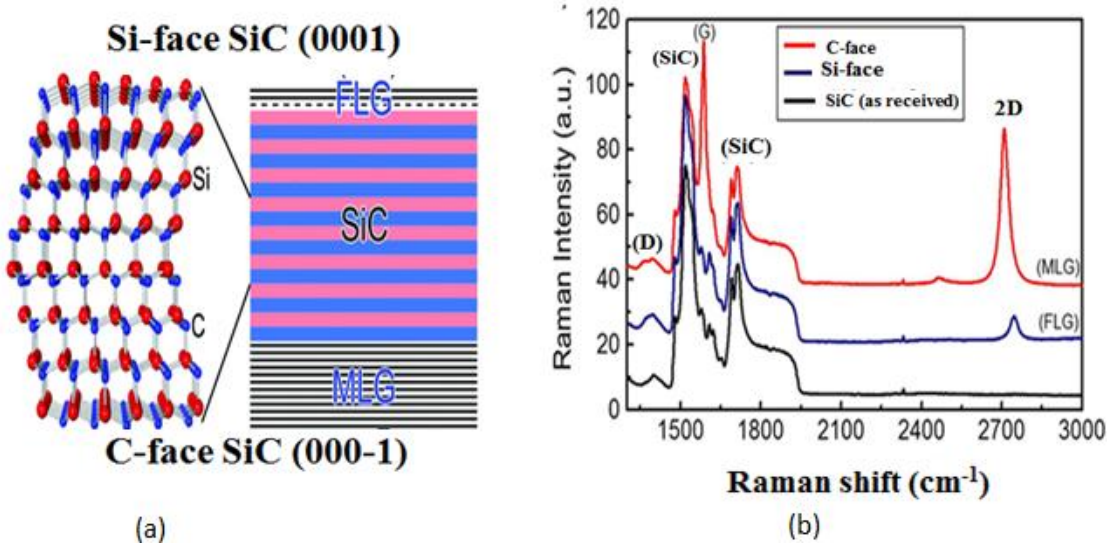

Figure 3.5. (a) few layers graphene (FLG) view on Si-face SiC, multilayer graphene view on C-face. (b) Raman measurements on C-face and Si-face SiC, the highest and the lowest 2D peaks correspond to multilayer and few layer graphene on C-face and Si-face respectively.

3.3.3. Controlling Graphene Growth Rate On C-face SiC

Excellent electronic properties of graphene opens opportunities to graphene based electronic devices. Epitaxial graphene grown on SiC is the most promising form of graphene for this purpose, but epitaxial graphene produced by conventional methods is of poor quality [10, 21]. Therefore much higher quality material should need to be produced for graphene based electronic devices applications.

Earlier electronic transport measurements were performed on epitaxial graphene films grown by UHV sublimation method. Graphene films produced in this way are defective and have low motilities $\mu \sim 15$ $cm^2V^{-1}s^{-1}$ [21, 23, 10]. Defects in UHV sublimated SiC referred to relatively low growth temperature and high graphitization rate in the out of equilibrium. UHV sublimation process and increasing growth temperature will anneal vacancies and grain boundaries. UHV growth method leads to unacceptable high sublimation rates especially on the C-face of SiC. A numbers of studies were focused on controlling the rate at which Si atoms sublime (for example by supplying Si in a vapour phase compound or by flowing an inert gas over the hot SiC surface [10, 21]). In this thesis work I discussed two different techniques which have been used to slow down epitaxial graphene growth rate in UHV conditions.

One of these methods called as confinement controlled sublimation technique (CCS), which was developed at Georgia institute of technology (GIT). We applied another technique which called as capping method .We developed the capping method in our laboratory at Izmir Institute of Technology.

The main idea of the Confinement controlled method developed at GIT based on restricting or confining the SiC in graphite enclosure (either in vacuum or in an inert gas).This method lead to maintains a relatively high Si vapour pressure on SiC surface to suppress the evaporation of Si atoms from SiC surface. Maintaining high Si vapour pressure makes growth of the garphene closed to thermodynamic equilibrium as shown in figure (3.6) [10].

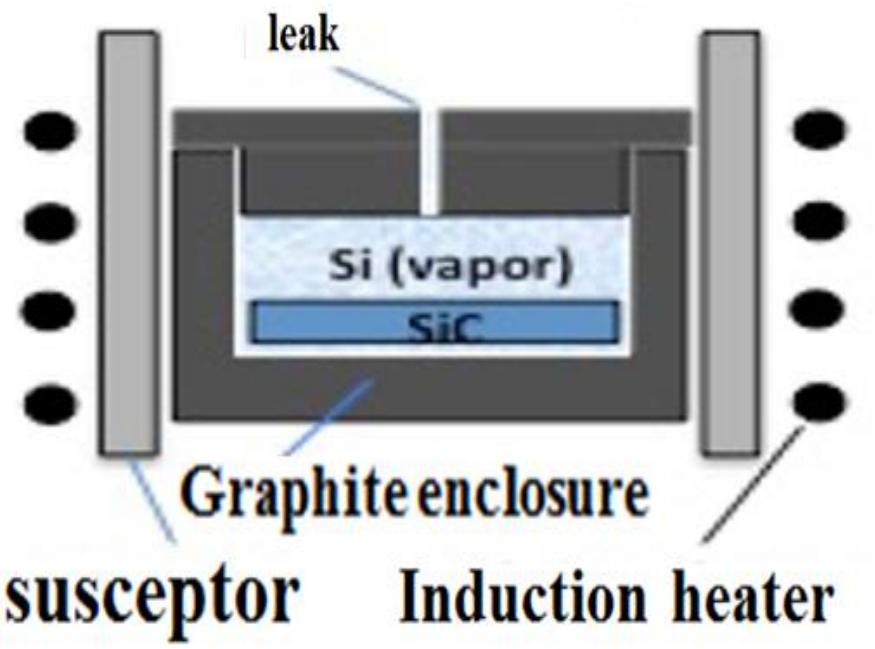

Figure 3.6. Confining SiC in graphite enclosure system

The principle of CCS can be understood from the kinetic gas theory [46]. Graphene growth rate is proportional Si depletion rate from the SiC surface. If Si evaporation rate (n^-) and condensation rate (n^+) are equal, then the two rates are exactly balanced (thermodynamic equilibrium).As long as evaporation and condensation rate are equal, graphene will no longer form. This condition established in hermetically sealed, non-reactive, enclosure at any temperatures after the enclosure surface have been passivated. Graphite enclosure and the passivation of the enclosure are achieved after several graphene growth cycles.

If Si atoms condenses on the surface with a sticking probability of ε, ($0 \leq \varepsilon \leq 1$) then,

$$n^+ = \varepsilon \nu_{ave} \rho_{eq}/4 \qquad (3.1)$$

Where ν_{ave} average thermal speed of Si atom in the vapour ($\sqrt{8KT/\pi m}$) ,ρ_{eq} is vapour density of Si in equilibrium with SiC at temperature T, and m is atomic mass. Sticking coefficients depend on the local surface structure. ε assumed to be 1 and independent of T and the growth rates on C-face are observed to be greater than the growth rate in Si-face this implies that ε is greater on the C-face and smaller on the Si-

face which is important for certain implementation of this method. Si atoms escape through the formed layer depends on graphene thickness. If $n^+ = n^-$, graphene will not form, but if some leak happened by applying small leak area in order to create difference between n^+ and n^- , some Si atoms will leave the enclosure through the leak. Then graphene can be form according to the graphene growth rate which is given by,

$$n_{gr} = n^- - n^+ \tag{3.2}$$

It is clear that n_{gr} is controlled by the size of the leak and as well as the number of the Si atoms evaporated from the SiC surface. The rate at which Si atoms sublime form is given by,

$$N = A\, v_{ave}\, \rho_{eq} \tag{3.3}$$

Where C is effective area of the leak (for cylindrical hole of D and length L, $A=D^3/3L$) and then consequently.

$$n_{gr} = N/A' \tag{3.4a}$$

$$n_{gr} = \nu_{ave}\, \rho_{eq\,(C/A)} \tag{3.4b}$$

Where A' is crystal surface area.

In the CCS experiment it has been found that for 1 cm^2 crystal in a vacuum with L =1cm and D=0.75 mm the graphene formation rate is reduced by more than a factor of about 10^3 when compared to UHV sublimation method in which $n^+=0$. After the experiment, AFM measurements have been carried out for bare SiC, C- rich face and Si-rich face as shown in figure (3.7).

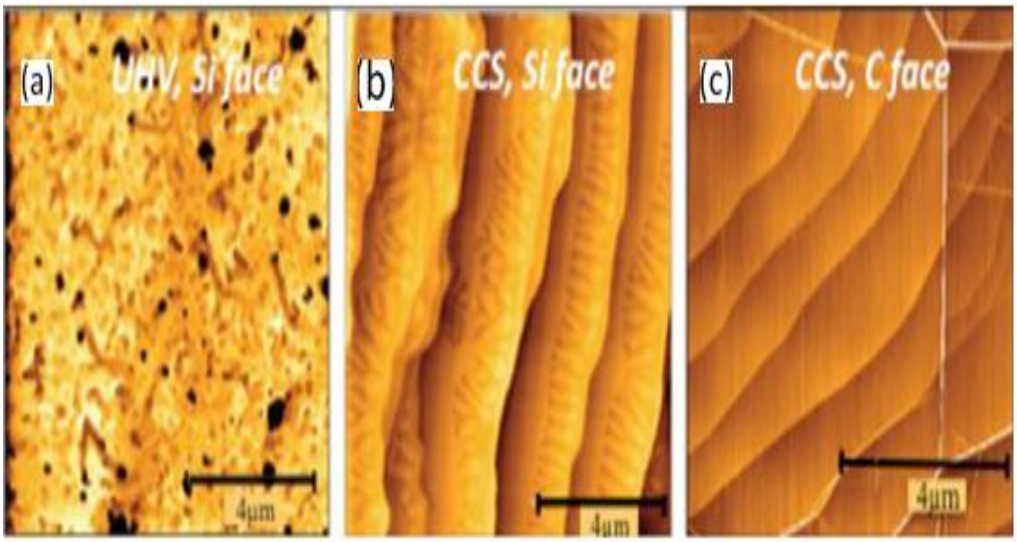

Figure 3.7. CCS AFM measurements (a) UHV, Si-face (b) CCS, Si-face (c) CCS, C-face [10].

The method that we have developed, a SiC substrate is capped by another SiC, as shown in figure (3.8).Our method is different from CCS but both two helped to reduce the number of the graphene grown layers on C-face SiC. Figure (3.8) shows our growth design in which the primary SiC substrate is capped by another SiC that was used as cap substrate. Our design provides a permanent small leak area between primary SiC and SiC cap substrate.

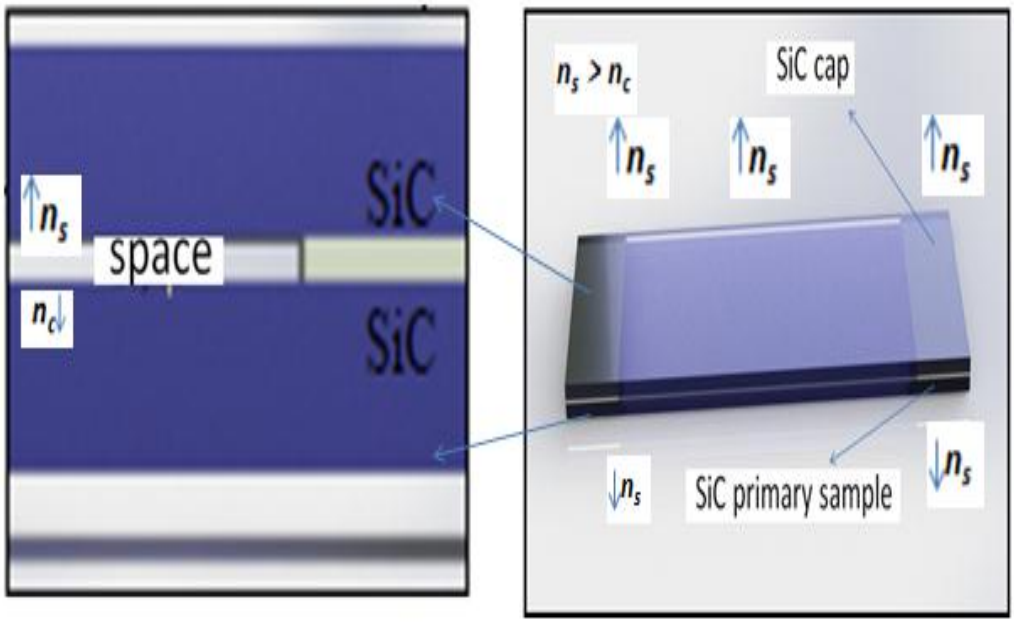

Figure 3.8. The schematic representation of the capping method.

This small leak area interrupts the thermodynamic equilibrium state between two substrate, and hence provide a permanent leak area from which Si atoms leave the surface giving a chance to form graphene. In our design, sublimation rate (n_s) and condensation rate (n_c) will never be the same, and the growth rate (n_g) is given by,

$$n_g \propto \nu_{avg} \rho \left(\frac{A}{S}\right) \tag{2.5}$$

Here ν_{avg} is average thermal speed of Si atoms, ρ is vapour density on SiC, A is leak area and S is sample surface area.

If we compare the equation (3.5) of capping method with the equation (3.4b) of CCS method, it can be found that the two equations are equivalent and the growth rate depends strongly on the vapour density of the Si atoms and as well as the average thermal speed of the Si atoms.

For the experiment we used 226μm thick on-axis and n-type (the doping concentration of approximately 10^{18} cm^{-3}), 4H-SiC wafer with epi-ready flat surface that was prepared by NovaSiC. The wafers were diced into 4mm wide and 10mm long rectangular substrate and cleaned chemically. The native oxide layer on the sample was removed in diluted HF solution prior to loading into the UHV chamber which has a base pressure of P = 1×10^{-9}mbar. The sample annealed in UHV by direct current heating during which the temperature is measured and controlled with an optical pyrometer. The sample degassed overnight at around 600 ˚C. Before capping the primary sample, The cap substrate is annealed to 1500 ˚C for about 1minute to eliminate any possible contamination[11], while the chamber pressure was measured to be P = 2×10^{-9} mbar during the annealing process. The cap substrate placed on top of the primary substrate as shown in figure (3.8), and then loaded into the UHV and annealed to 1500 ˚C for 1 minute. After the annealing process we performed Atomic Force Microscopy (AFM) measurements first on bare SiC then capped sample, and on C-face UHV exposed sample .The results of the measurements is in the following figure (3.9).

In general CCS and capping methods are two methods, used to control epitaxial graphene growth rate, the two methods are based on making different between sublimation and condensation rate. Moreover CCS method and capping methods lead to reduction of a graphitization phenomenon (carbonization rate) which is in turn leads to more uniformity and homogeneity in garphene grown layers and opened a new ways to produce high quality graphene both in single layers and multilayers.

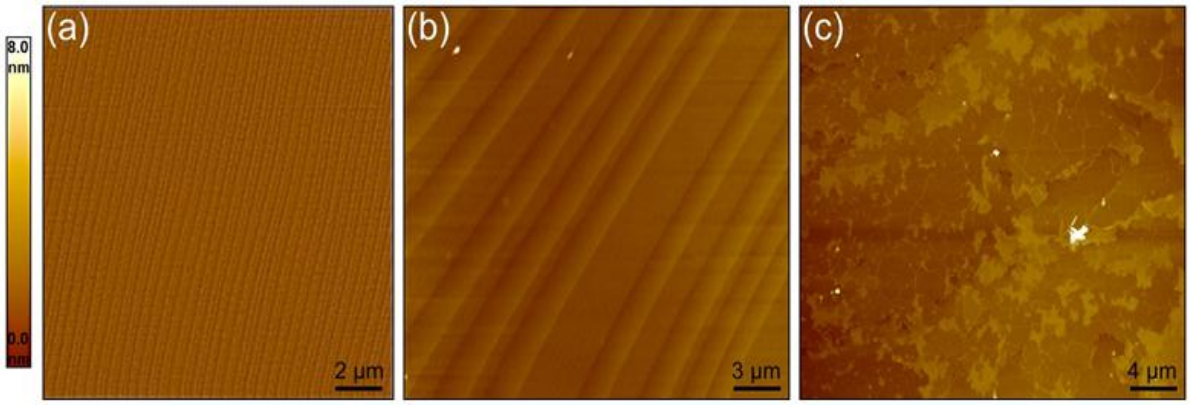

Figure 3.9. AFM measurements (a) SiC as received, the width of the terraces approximately is .0.5 and .06 µm. (b) C-face SiC primary substrate after high temperature annealing , during the annealing process he terraces width broadened to approximately 3 to 5 µm and height of 2 nm (c) AFM topography on C-face UHV expose uncapped sample surface .

CHAPTER 4

EXPERIMENTAL

4.1. Experimental Setup

In this section we will take a look at the experimental setup that we have used it to perform the experiments, sample preparation and the results of the carried experiments. The setup consists of two main parts which are sample stage (sample holder) and the chamber (ultra-high vacuum system UHV).

4.1.1. Ultra-High Vacuum System (UHV)

UHV is a vacuum system charactrized by pressure lower than 1×10^{-9} mbar (100 nanopascal). Reaching such a pressure requires specific material , pumps and it dose also require heating the entire system above 100 ˚C for many hours (callede baking) in ordre to remove the water and the gases that adsorb in the inner surface of the vacuum chamber. UHV is necessary for scientific researches and researchers those who work in a modern technology especially epitaxial growth of a nano-films, thin film deposition and surface science techniques.

All experiments are done in our UHV system which extremely needed for the purpose of growing epitaxial graphene. In order to achieve UHV some initial and special procedures are needed. Firstly dry pump is used as roughing pump to remove the small particles as the dust and other particles that ca be presented in the surface of chamber. The roughing pump takes the system down to 10^{-2} mbar. After reaching approximately 10^{-2} mbar or a bit lower pressure and in order to reach ultra-high vacuum level, a turbo-molecular is used to take whole the system down to low 10^{-9} mbar range ,figure (4.1) shows UHV system and its components where the experiments are done.

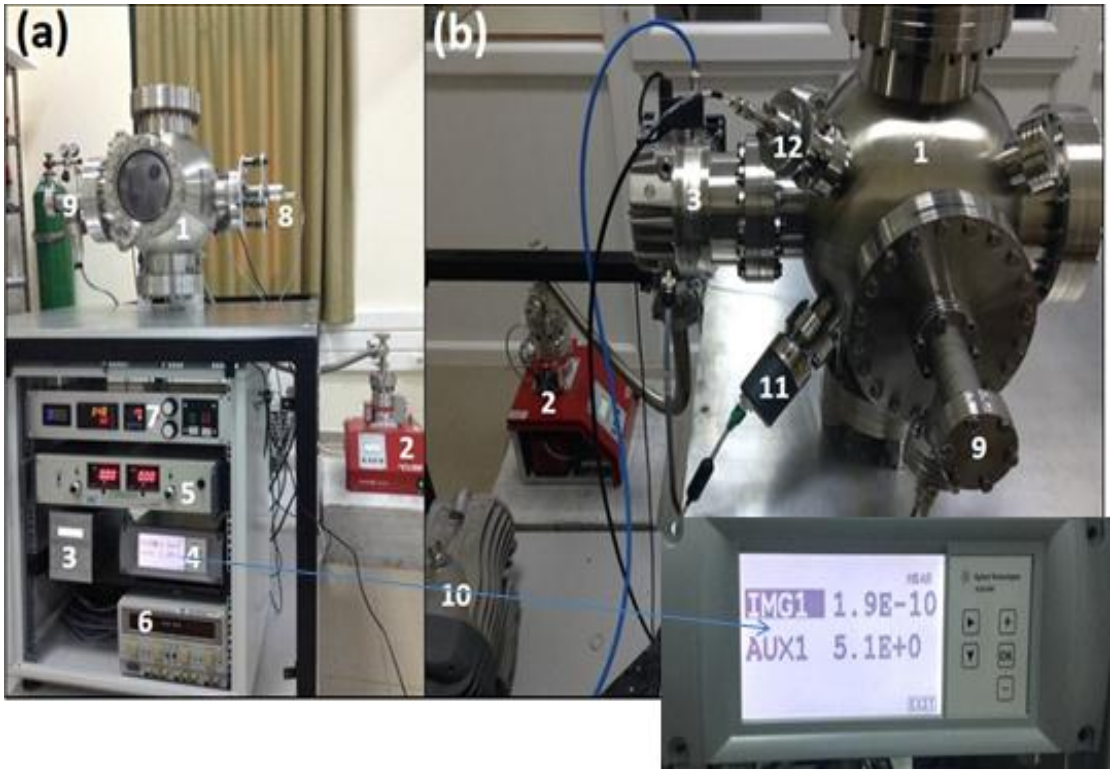

Figure 4.1. UHV chamber and its control units(1) UHV chamber(2)Hi-cube pump which takes the system down to the low vacuum level (3)turbo-molecular pump and its control units, turbo-molecular pump is use to reach ultra-high vacuum(10^{-9} mbar – 10^{-10}mbar)(4) Vacuum gauge control unit.(5) DC power supply.(6) another DC power supply.(7) temperature control panel (it reads the temperature inside the chamber and out the chamber by using thermocouple and its shows the pyrometer read as well).(8) optical pyrometer.(9) sample holder. (10) Scroll pump. (11) Cold cathode vacuum gauge (Varian FRG-700). (12) UHV vacuum gauge (Varian IMG-300).

4.1.2. Sample Stage

The second part of the system is the sample stage (sample holder) and it consist a parts which were chosen according to high temperature that occurs during the annealing process .The outer part is stainless steel and the internal parts are refractory materials like Tantalum(Ta) and Alumina Ceramic(Al_2O_3). Both Ta and Al_2O_3 parts, are the most demanding material that can be used in high temperature applications, for example the melting point of Ta and Al_2O_3 is 3020 ˚C and 2072 ˚C respectively. Al_2O_3 is also good for high temperature applications due to its excellent dielectric property, thus Al_2O_3 used to isolate the Tantalum plates from each other while annealing the

sample at high temperature. The sample stage we design for annealing our sample is shown in the in the figure (4.2)

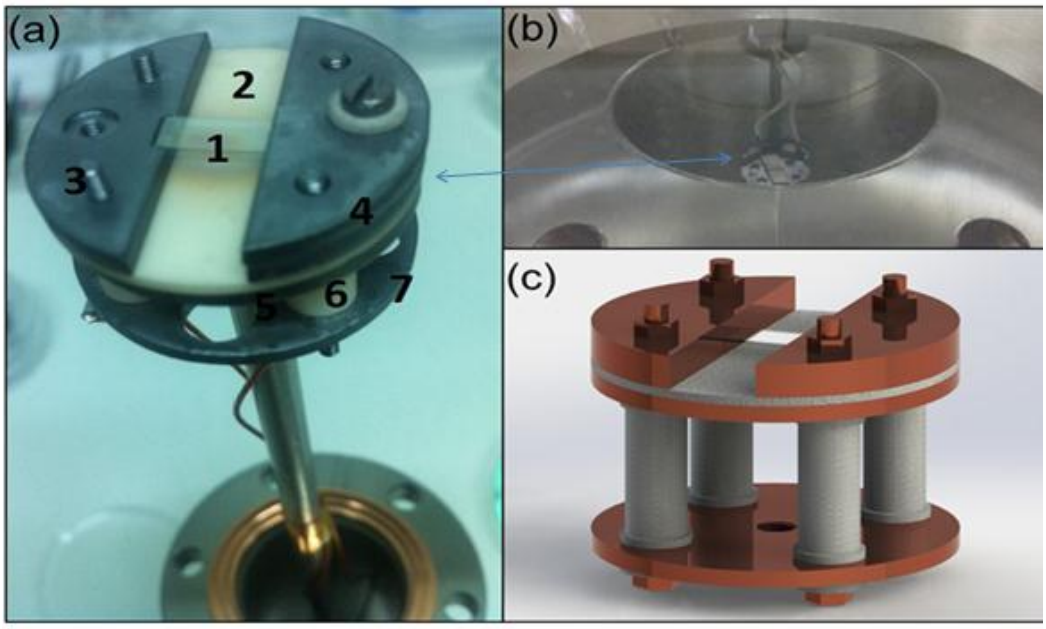

Figure 4.2. (a)sample stage(1)SiC wafer(substrate).(2)Alumina ceramic**(**Excellent dielectric properties from DC to GHz frequencies.(3)Tantalum screw (4) tantalum plates top of each other(5) upper Tantalum plate(6)another Alumina Ceramic(7) circular tantalum plate with holes and screw so as to hold the upper units which are contain the sample (b) sample stage from inside the chamber (c) sample stage 3D view.

After the sample placed in the sample holder as shown in the figure (4.2), it's connected to a power simply (see figure.4.1.Number5) which provides direct current and voltage to anneal the sample by direct current heating method.

4.1.3. Sample Preparation

Prior to loading the sample to UHV chamber, sample must be well prepared and cleaned. We used ultrasonic cleaning to clean the sample and the cleaning time taken between 3-15 minutes by using acetone and alcohol respectively. We used acetone because it's a very good solvent and it can dissolve almost all organic compounds from SiC substrate. After cleaning the sample by using acetone, alcohol used to remove the remaining acetone. Furthermore the native oxide layer on SiC is etched in a HF acid But even after the sample cleaned by HF oxide will recreate itself that's because of the

Oxygen in Air, therefore for further oxide removal the sample heated inside the vacuum chamber up to 1150 ˚C (the preparation and graphene growth procedures are summarized in the table 1 part 4.2).

4.2. Growth of Epitaxial Graphene: Experimental Techniques and Parameters

For the experiment we used 226μm thick on-axis and n-type (the doping concentration of approximately 10^{18} cm^{-3}) 4H-SiC wafer with automatically flat surface that were prepared by NovaSiC. The wafer were diced into 4mm wide and 10mm long rectangular substrate and cleaned chemically. The native oxide layer on the sample was removed in diluted HF solution prior to loading into the UHV chamber which has a base pressure P of 1×10^{-9}mbar. the sample annealed in UHV by direct current heating during which the temperature is measured and controlled with what's called pyrometer.in our experiment the sample degassed overnight at around 600 ˚C and the reaming surface oxide was removed thermally by annealing the sample for about 10 minutes at 1100 ˚C (the preparation and graphene growth procedures are summarized in the table 1)

Table 4.2.1 preparation and graphene growth procedures.

Temperature	Time (minutes)	Purpose
600 ˚C	Overnight	Thermal cleaning
1050 ˚C -1100 ˚C	10	Oxide removal
1300 ˚C -1350 ˚C	6-7	Surface preparation
1450 ˚C -1500 ˚C	1-10	Graphene growth

After last step (1450 ˚C -1500 ˚C) in the table above whole the system cooled down and the sample removed from UHV system and got ready to study by surface science technology (scan probe microscopy techniques) and Raman spectroscopy.

4.3. Characterization Methods

After graphene grown on top of SiC substrate, the samples are characterized by Raman spectroscopy, atomic force microscopy (AFM) and optical microscope.

4.3.1. Raman Spectroscopy

Raman is a useful method to study the doping, defects, disorder, number of layers and associated strain in graphene. Raman spectroscopy considers a quick way to detect the presence of graphene. Raman spectrum of epitaxial graphene consists of three main bands (peaks) known as G, D and 2D which are well characterized and understood.

We performed Raman spectroscopy measurements for the samples annealed up to 1450 ˚C for about one minute in UHV chamber with a pressure of 2×10^{9}mbar .The measurements were conducted by using a green laser of 532 nm wavelength. But before performing Raman measurements for annealed sample, we performed Raman measurements on bare SiC in order to recognize the difference with and without annealing. Raman spectra of epitaxial graphene on SiC have three band peaks which are 2D, G, and D. Figure (4.3b) depicts the Raman spectra of epitaxial graphene and their positions. The presence of D peaks in our measurements is due to local defects and disorders in the grown layers and the low intensity of this peak shows that there is only small amount of defects/disorder in epitaxial graphene grown layers [37, 38] G peak derived from in-plane motion of the C atoms and appears nearly at $1600cm^{-1}$ position [36]. 2D band also (also called G') band, appears approximately at the position of $2700cm^{-1}$ or a little bit less depending on the garphene layers number [37, 39]. 2D in graphene is related to second order two phonon process and exhibits an unusually strong frequency dependence on the excitation laser due to double resonance process which links the phonon wave vector to the electronic band structure. Generally, the appearances of 2D and G peaks due to double resonance electron phonon process.

As seen in fig (4.3b) 2D in in the C-face grown graphene has high intensity compare to the one in Si-face grown graphene this show that the number of graphene layer on C-face SiC is larger than the one in Si-face SiC.

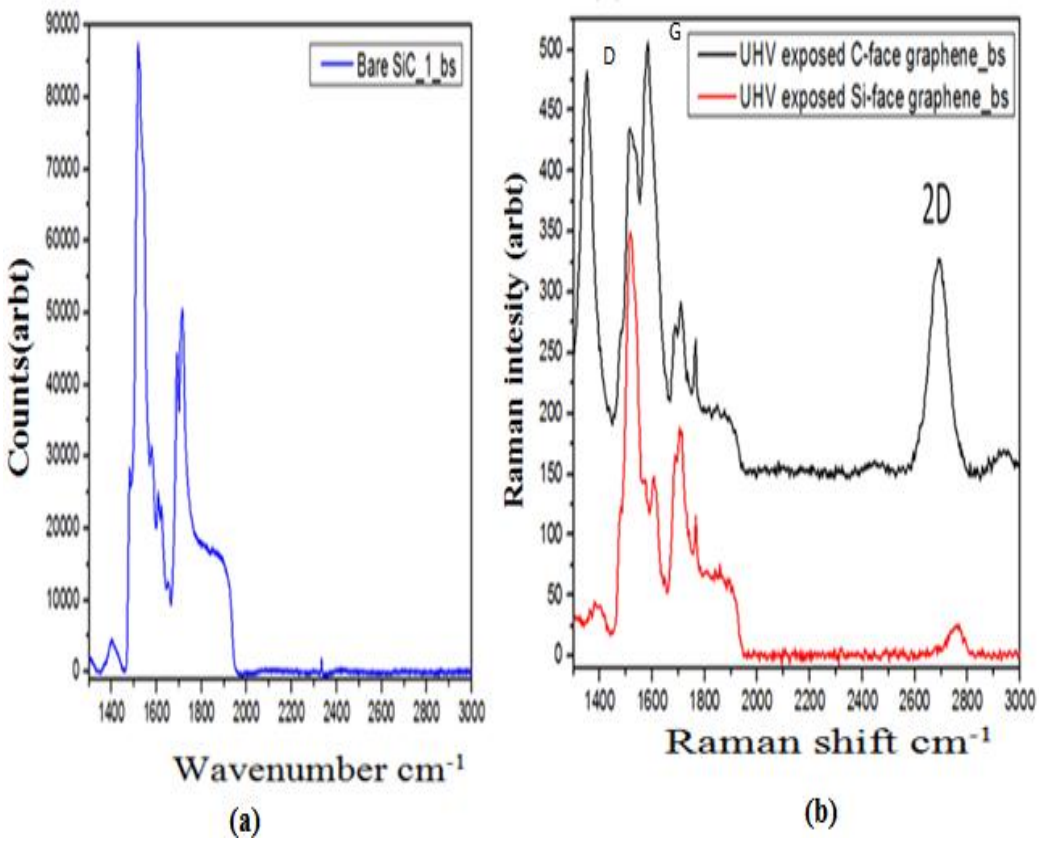

Figure 4.3. Raman measurements on bare SiC and on both Si-face and C-face contains graphene grown epitaxially after the sample annealed to 1450^{o} C for about one minute (a) Raman spectra of bare SiC (b) Raman spectra of epitaxial graphene showing D,G and 2D peaks positions

As seen in figure (4.3b) 2D in in the C-face grown graphene has high intensity compare to the one in Si-face grown graphene this show that the number of graphene layer on C-face SiC is larger than the one on Si-face SiC .

In order to show how the intensity of 2D peak been impacted by epitaxial graphene layers grown in SiC, we performed another experiment in which UHV exposed sample annealed up to 1500 ˚C for about 1 minute and base pressure was about 2.0×10^{9}mbar. We performed Raman measurements in C-face that because the growth rate in this face faster than Si-face. The measurements performed at the areas marked as 1, 2 and 3 shown in figure (4.4a) which shows C-face optical image.

It's clear that in the area number 3, 2D peak has high intensity due to strong interaction between electrons and phonons (electron phonon mode) in contrast with areas 1and 2 which are contain few layer epitaxial graphene compared to area 3.

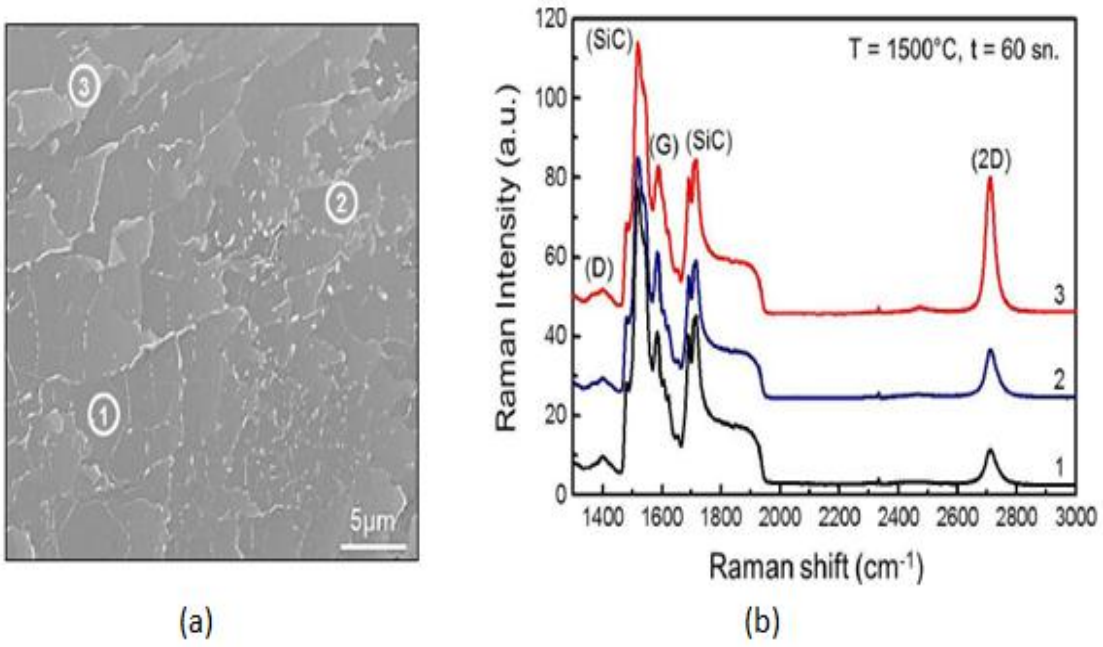

Figure 4.4. (a) C-face optical microscope image (b) Raman measurements at the areas 1, 2 and 3, representing few layers and multilayers epitaxial graphene respectively.

4.3.2. Raman Spectroscopy Analysis of Epitaxial Graphene

We examined how epitaxial graphene grown layers depend on time and temperature, for this purpose experiment carried out, in which C-face SiC samples annealed for 1, 3 and 5 minutes at 1400 ˚C and 1550 ˚C separately . Three different Raman measurements at 514 nm were taken at centres of the surfaces and two at the point's 250 μm away from the centres. Acquired Raman signals were compared to the measurements from literature by means of shape, width (FWHM) and position [18]

In figure (4.5) and (4.6), Raman measurements were taken on C-face SiC for two groups of SiC substrates, in group one SiC substrates annealed to 1400 ˚C annealed for 1, 2, 3 and 5 minutes. In Group two, SiC substrates annealed to 1550 ˚C for the same time as in group one, the acquired results of the measurements compared.

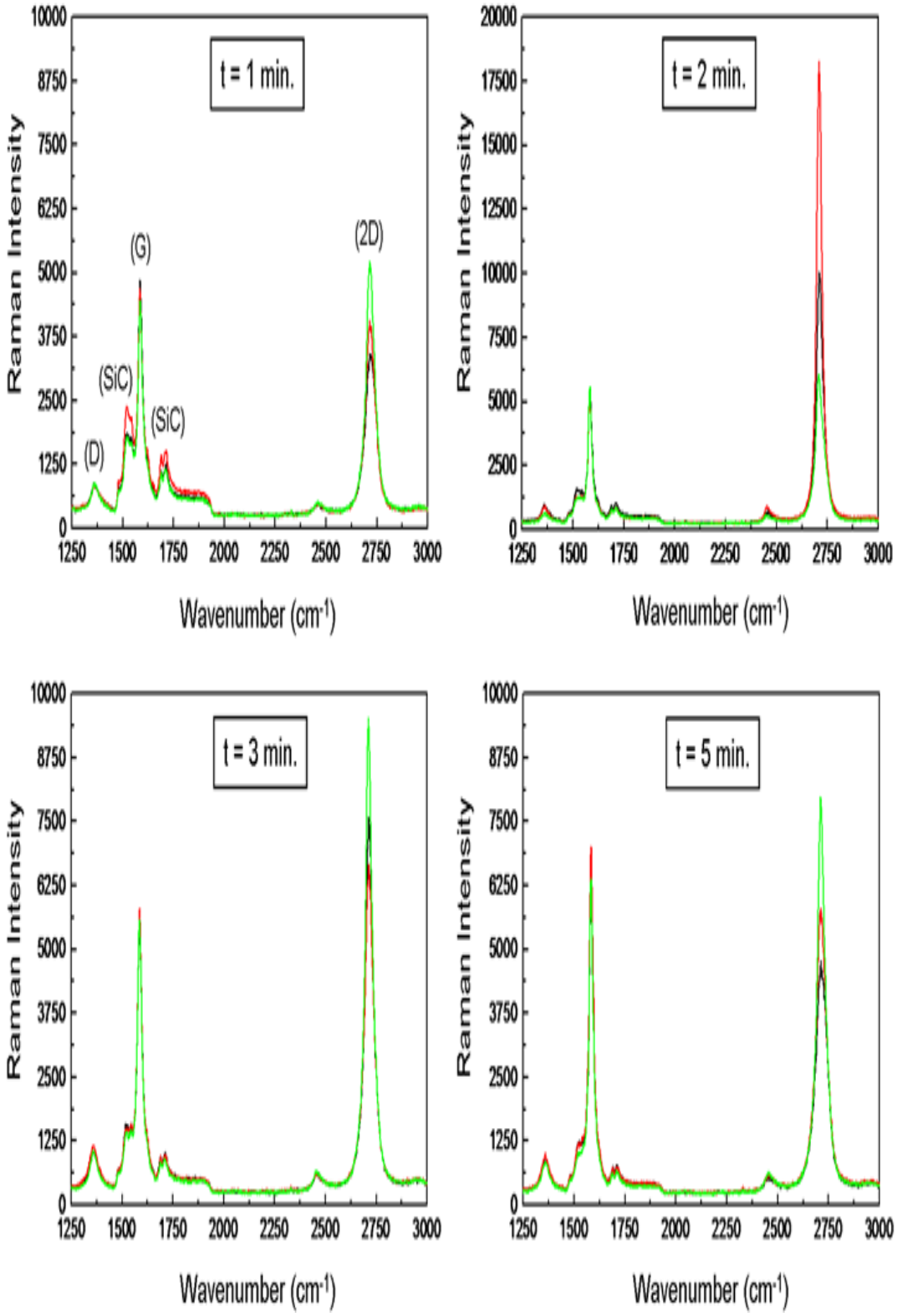

Figure 4.5. Raman measurements on C-faces SiC substrates annealed to 1400 ˚C for different period of time.

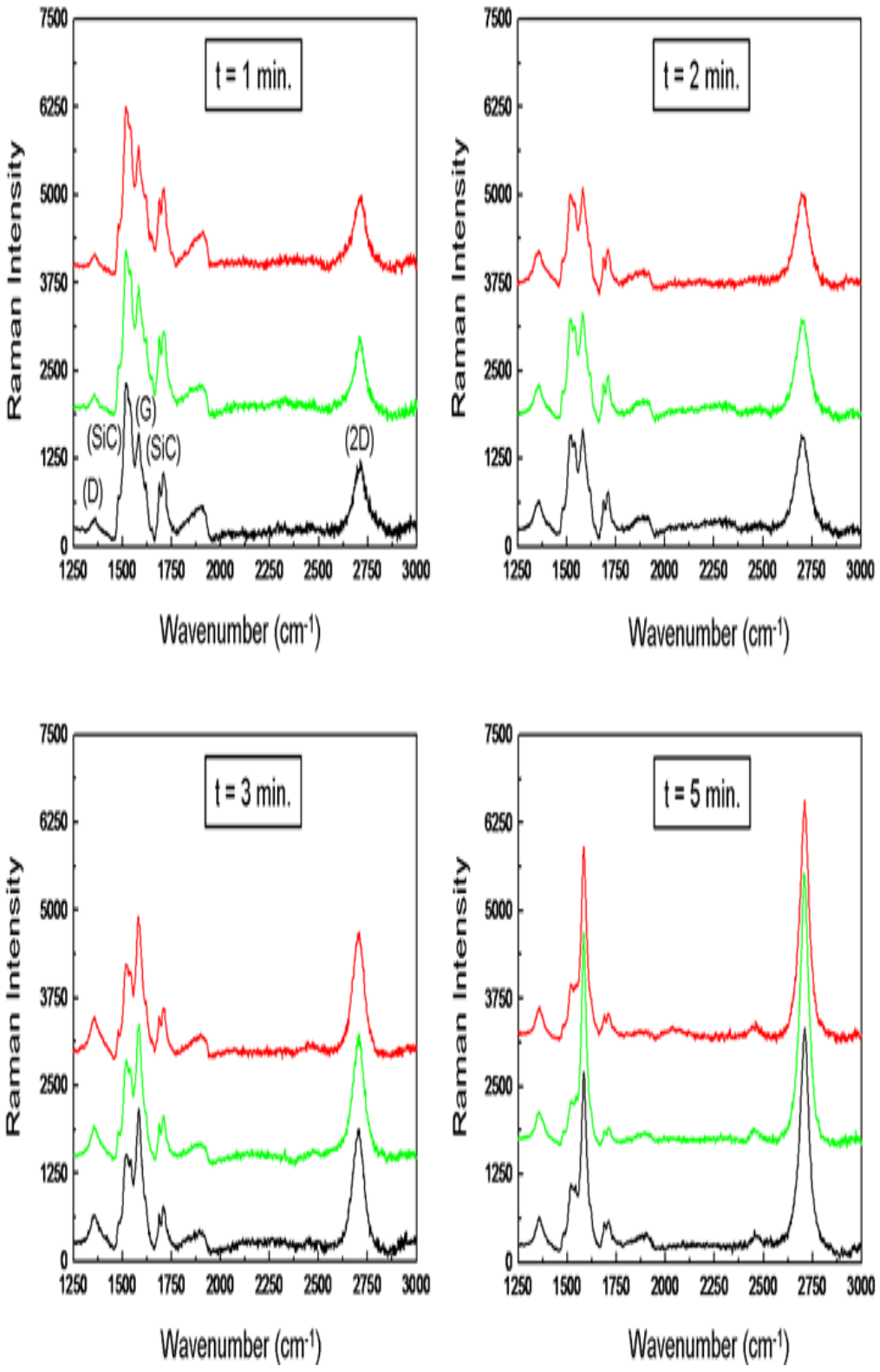

Figure 4.6. Raman measurements on C-faces SiC substrates annealed to 1550 ˚C for different period of time. Different colour corresponds to single point Raman measurements on different spot on the sample

Both Raman measurement results obtained for two groups show that as the growth time increases the SiC signal decreases and G-band and 2D-band peaks connected to graphene/graphite increases. The decrease in SiC signal and the increase in 2D peak indicate that the amount of graphene layer increases as the time increases. It is seen that the increase in the amount of layers at 1400 ˚C is unequal and unregulated when compared to the samples annealed at 1550 ˚C. In addition, the Raman measurements taken at 250 μm away from the center of the sample let us confirm that graphene/graphite thickness changes differently and disorderedly for different points for the samples annealed at 1400 ˚C. Even though it is possible to address the amount of graphene layers that are acquired by mechanical separation processes, by using Raman spectroscopy at the precision rate of one layer, the same method does not let the epitaxial graphene layers on SiC surface be determined as precisely. The layer amount of epitaxial graphene can only be determined by techniques such as X-ray diffraction and photoemission spectroscopy [18].

4.3.3. AFM Measurements

For a UHV exposed sample annealed up to 1400 ˚C for about 10 minutes the morphology of the annealed sample surface is analysed by AFM measurements (We analysed AFM measurements by using Nova-scan a software analyser for scan probe microscope measurements) and the results are compared with the ones obtained from as-received SiC surface as illustrated in figure (4.7a), as-received sample surface is dominated by 0.5-0.6μm wide, well ordered and automatically flat due to approximately 0.1˚ miscut of the wafer. These terraces are created during the preparation of the epi-ready SiC surface. After the annealing process, we found 1-4 μm wide stepped terraces separated by oblique step edges, whose height range depending on the width of the terrace see figure (4.7b), Such a modification of the surface is not related to the formation of graphene but due to the annealing of SiC crystal.

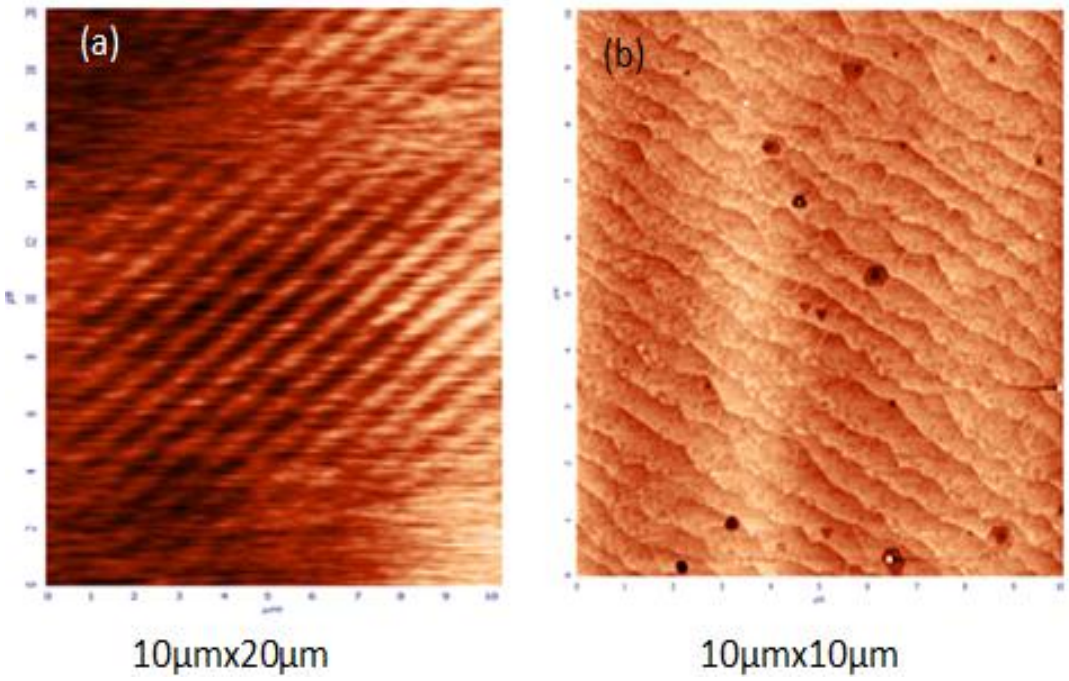

Figure 4.7. (a) AFM of SiC as received sample (b) morphology of the sample after annealing process.

Furthermore we took a cross section over the surface (selected randomly) to determine the height and the width of the terraces [see figure (4.8)].

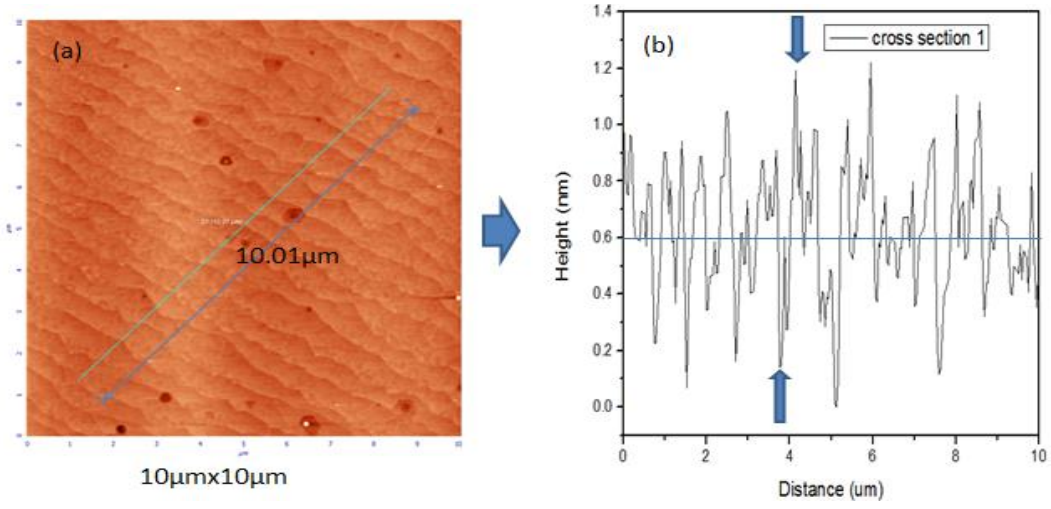

Figure 4.8. (a) Cross-section taken randomly in the are we called high 1 (b) analysed data which correspond to cross section taken in (a), origin program used to analyse the data in order to determine the height and the width of the terraces .

The height of the terraces can be determined by subtracting the minimum value of the signal from the AFM maximum value. For example the height a signal terrace shown in figure (4.8 b) approximately 1.05 nm, this result is obtained by subtracting the minimum and the maximum of the AFM signal. From these analyses we found that the average height of each terrace is about 0.6nm. Therefore we conclude that atomic terraces are formed during the annealing process.

As it is mentioned before the terraces are formed as the result of the annealing process, beside that the annealing process leads to grains structure on SiC surface as depicted in figure (4.10).

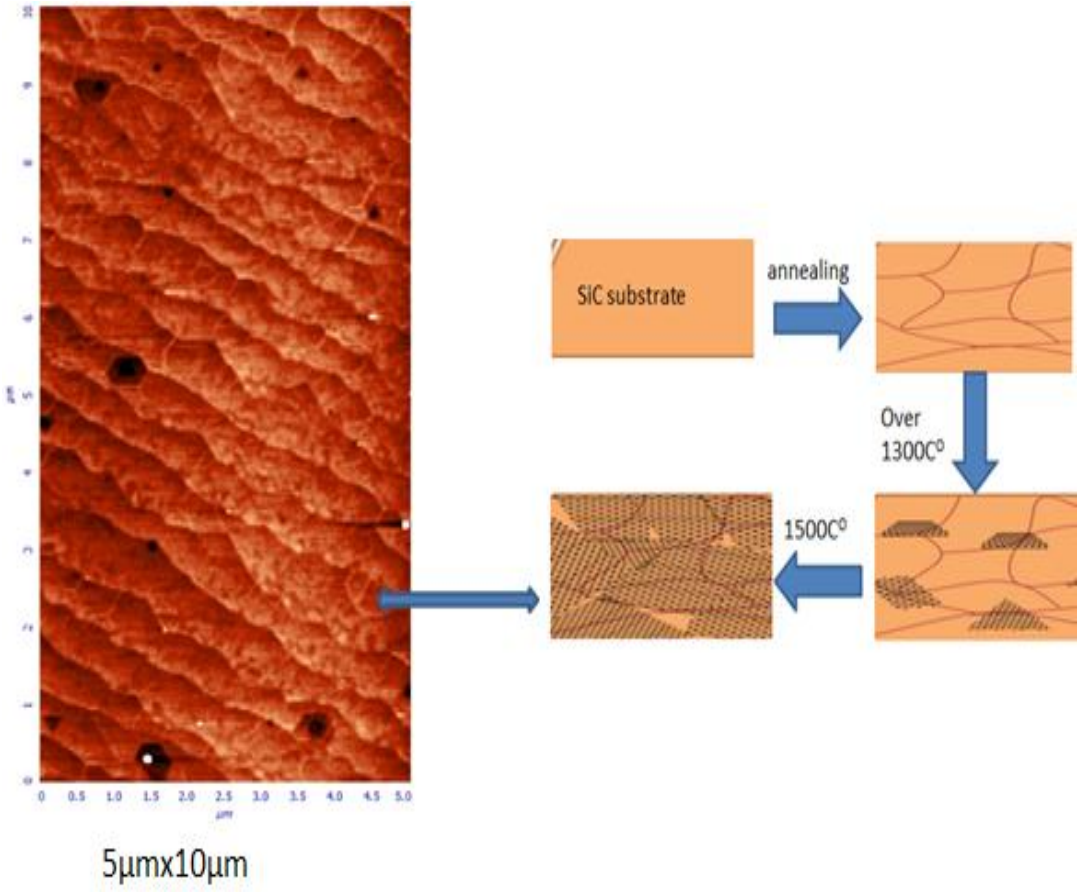

Figure 4.9. AFM image of the annealed SiC surface retaining the grains.

Grains growth could be understood from the effect of temperature on metal formation principle [see figure 4.10] below [17].

During the recovery some of the stored internal strain is no longer distressed by virtue of dislocation motion (in the absence of externally applied stress, as result of enhanced atomic diffusion at the elevated temperature [17].

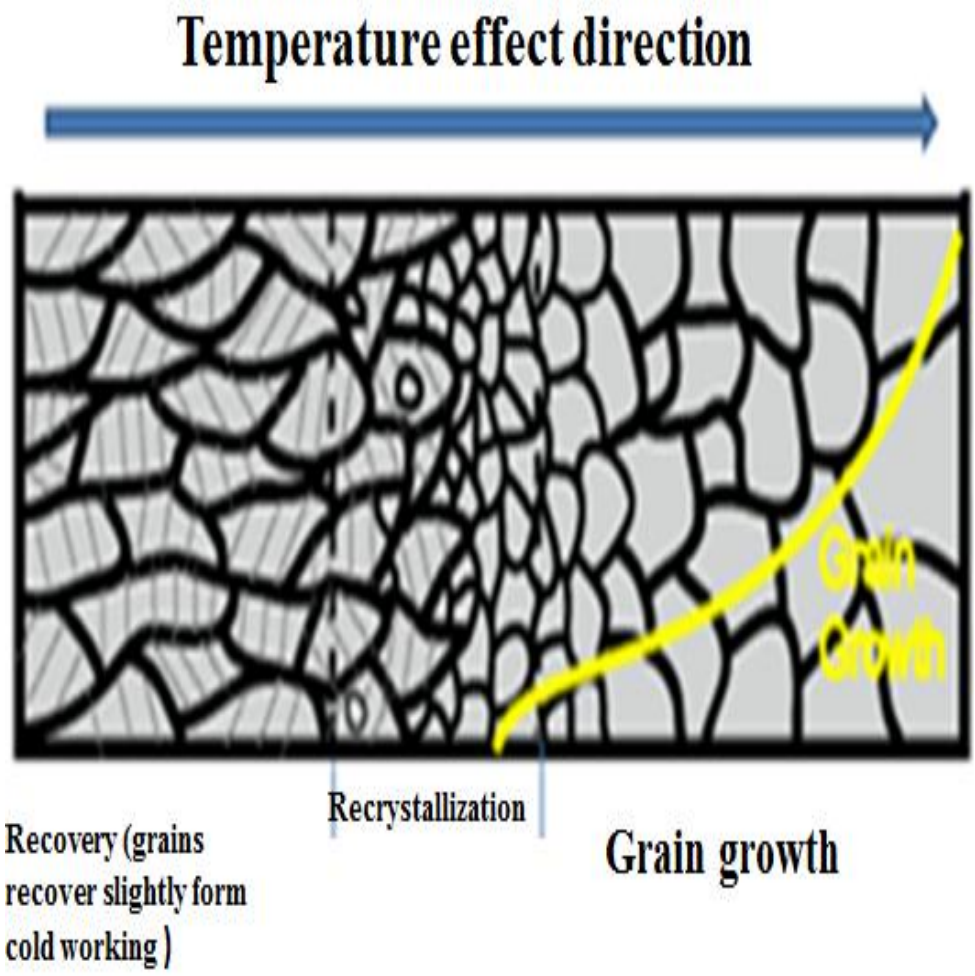

Figure 4.10. The effect of temperature on the crystal formation.

Even after recovery complete the grain still in a relatively high strain energy state. The next stage to recovery is the Recrystallization which is consider as formation of a new set of strain and sometimes have approximately equal dimensions in all direction .This new grains structure have been formed as result of the differences in internal energy between strained and un-strained material. The new grains form as very small nuclei and grow until they completely consume the parent material [17], but in the case of epitaxial graphene on top of SiC, consuming the parent material is not welcoming process because such a process lead to bulk graphite instead of epitaxial graphene. Recrystallization is process depends on both time and temperature while the degree or fraction of it increase with time where the influence of temperature is demonstrated in the figure (4.10). The Recrystallization proceeds more rapidly in pure metal than in alloys and as mentioned elsewhere during recrystallization, grain boundary motion occurs as new grain nuclei form and then grow. grains appearance in

SiC after was annealed up to 1500 ^{o}C.it tell or give an indication of a new material formed on the surface which is graphene in the case of annealing SiC .The fast way to test the presence of a graphene its by carrying out Raman measurements because it's a very quick way to detect its presence [see the figures (3.6b), figure (4.3) and figure (4.4).

CHAPTER 5

CONCLUSIONS

In this thesis work we worked and focused in graphene as a new material that expected to change the map of the future electronic application. In chapter 1, we have given a definition to graphene, we reviewed its lattice unite vectors $\vec{a}_1$ and $\vec{a}_2$,the nearest neighbors δ_1, δ_2 and δ_3 vectors furthermore we discussed its first brillouin zone and the locations of Dirac points K and K′ in the first brillouin zone.

In chapter two we discussed electronic structure and physical properties of graphite and graphene. We showed how graphene band gap different from the band gap of the typical semiconductors. We showed the charge carries behave as massless in graphene, as result graphene has zero band gap while the dispersion is linear around the point where the conduction and the valence band meet., in this chapter we discussed an earlier attepmts to synthesis graphene such as graphite intercalation methods by inserting molecules or atoms in between graphite layers aiming to separate graphite layers. there are recent methods such as chemical vapour depositoin(CVD) and mechanical cleavage used to obtain graphene, in this thesis work, CVD briefly discused and we obtained graphene by using micromechcanical cleavage method and we charaterized the results by Raman spectrocopy.

The successful development in garphene-based electronic devises depends on the large scale production of the graphene material and slowing graphene growth rate. The preparation of a single layer or few layers graphene grown epitaxially by the thermal decomposition of SiC has been proposed as a viable route for the synthesis of uniform, wafer-size graphene layers for technological applications. Therefore in chapter 3 we focused on epitaxial graphene and its growth on SiC on Ultra-high vacuum (UHV) system. Since graphene grow epitaxially on SiC we have discussed SiC and its polar surface then we showed the mechanism of the graphene growth on SiC surface. SiC has two typical orientations of surfaces, Si-rich (0001) face which is terminated by Si atoms and the other one is C-rich (000-1) face which is terminated by C atoms, we grow graphene on both faces and we showed how the two faces are different in term of the

numbers of the layers grown on each face , the results showed that graphene grows on C-face with the growth rate faster than that on Si-face and in turn we reviewed two different methods used to slow the growth rate on C-face, one developed at Georgia institute of technology (GIT) and we developed called capping method , both two methods succeed in slowing the growth rate of graphene on C-face. Finally, in chapter 4 we discussed our experimental setup including UHV system, sample stage (design and components) and sample preparation .The last part of chapter 4 was about experimental techniques, parameters and characterization methods (Raman measurements and AFM measurements). We analysed AFM images by using Nova software then we abled to determine the height and the width of the terraces that created on SiC surface.

Since graphene on C-face grows faster than that on Si-face, we used capping method to reduce the growth rate of epitaxial. By using the results obtained from AFM measurements, we explained the difference between capped sample and uncapped sample. The developed capping technique increases the probability of using epitaxial graphene on C-face of SiC for two dimensional electronics applications.

Temperature and growth time dependence of epitaxial graphene are analysed by using Raman spectroscopy measurements. Our measurements showed that the number of graphene layers increases as the growth time goes on for the same growth temperature. The terraces formation on SiC during the annealing process has been analysed by AFM measurements. The topography of SiC surface is studied before and after the annealing process .The obtained images depict that epitaxial graphene covers the entire SiC surface as the terrace structure forms during the annealing process

REFERENCES

[1] Wang, C., Li, J., Amatore, C., Chen, Y., Jiang, H., & Wang, X. M. (2011). Gold nanoclusters and graphene nanocomposites for drug delivery and imaging of cancer cells. *Angewandte Chemie International Edition*, *50*(49), 11644-11648.

[2] A. K. Geim, K. S. Novoselov: *Nat. Mater.* **6**, 183 (2007).

[3] Xuebin Li. *Epitaxial Graphene films on SiC: Characterization and Devices*, Ph.D thesis presented at GIT august 2008 approved by W.D. Heer, T. Orlando and J.D. meindle April 2008.

[4] Sur, U. K. (2012). Graphene: A rising star on the horizon of materials science.*International Journal of Electrochemistry*, *2012*.

[5] Geim, A. K., & Novoselov, K. S. (2007). The rise of graphene. *Nature materials*, *6*(3), 183-191.

[6] Miao, C., Zheng, C., Liang, O., & Xie, Y. H. (2011). *Chemical vapor deposition of graphene*. INTECH Open Access Publisher.

[7] Seah, C. M., Chai, S. P., & Mohamed, A. R. (2014). Mechanisms of graphene growth by chemical vapour deposition on transition metals. *Carbon*, *70*, 1-21.

[8] Raza, H. (2012). *Graphene nanoelectronics: Metrology, synthesis, properties and applications*. Springer Science & Business Media.

[9] Real, M. A., Lass, E. A., Liu, F. H., Shen, T., Jones, G. R., Soons, J. A. ... & Elmquist, R. E. (2013). Graphene epitaxial growth on SiC (0001) for resistance standards. *IEEE Trans Instrum Meas*, *62*, 1454.

[10] De Heer, W. A., Berger, C., Ruan, M., Sprinkle, M., Li, X., Hu, Y., ... & Conrad, E. (2011). Large area and structured epitaxial graphene produced by confinement controlled sublimation of silicon carbide. *Proceedings of the National Academy of Sciences*, *108*(41), 16900-16905.

[11] Celebi, C., Yanık, C., Demirkol, A. G., & Kaya, I. I. (2012). The effect of a SIC cap on the growth of epitaxial graphene on SIC in ultra high vacuum. *Carbon*,*50*(8), 3026-3031.

[12] Misra, P. (2011). *Physics of condensed matter*. Academic Press.

[13] Novoselov, K. S. (2011). Nobel lecture: Graphene: Materials in the flatland.*Reviews of Modern Physics*, *83*(3), 837.

[14] Geim, A. K., & Novoselov, K. S. (2007). The rise of graphene. *Nature materials*, *6*(3), 183-191.

[15] Dresselhaus, M. S., & Dresselhaus, G. (2002). Intercalation compounds of graphite. *Advances in Physics*, *51*(1), 1-186.

[16] Greenwood, N. N., & Earnshaw, A. (2012). *Chemistry of the Elements*. Elsevier.

[17] Callister, W. D., & Rethwisch, D. G. (2012). *Fundamentals of materials science and engineering: an integrated approach*. John Wiley & Sons.

[18] Ni, Z. H., Chen, W., Fan, X. F., Kuo, J. L., Yu, T., Wee, A. T. S., & Shen, Z. X. (2008). Raman spectroscopy of epitaxial graphene on a SiC substrate.*Physical Review B*, *77*(11), 115416.

[19] Hass, J., Feng, R., Li, T., Li, X., Zong, Z., De Heer, W. A., ... & Berger, C. (2006). Highly ordered graphene for two dimensional electronics. *Applied Physics Letters*, *89*(14), 143106-143106.

[20] Norimatsu, W., & Kusunoki, M. (2014). Epitaxial graphene on SiC {0001}: advances and perspectives. *Physical Chemistry Chemical Physics*, *16*(8), 3501-3511.

[21] Forbeaux, I., Themlin, J. M., & Debever, J. M. (1998). Heteroepitaxial graphite on 6 H-SiC (0001): Interface formation through conduction-band electronic structure. *Physical Review B*, *58*(24), 16396.

[22] Emtsev, K. V., Bostwick, A., Horn, K., Jobst, J., Kellogg, G. L., Ley, L., ... & Seyller, T. (2009). Towards wafer-size graphene layers by atmospheric pressure graphitization of silicon carbide. *Nature materials*, *8*(3), 203-207.

[23] Berger, C., Song, Z., Li, T., Li, X., Ogbazghi, A. Y., Feng, R., ... & De Heer, W. A. (2004). Ultrathin epitaxial graphite: 2D electron gas properties and a route toward graphene-based nanoelectronics. *The Journal of Physical Chemistry B*,*108*(52), 19912-19916.

[24] Trabelsi, A. B. G., Kusmartsev, F. V., Robinson, B. J., Ouerghi, A., Kusmartseva, O. E., Kolosov, O. V., ... & Oueslati, M. (2014). Charged nano-domes and bubbles in epitaxial graphene. *Nanotechnology*, *25*(16), 165704..

[25] Gupta, A., Sakthivel, T., & Seal, S. (2015). Recent development in 2D materials beyond graphene. *Progress in Materials Science*, *73*, 44-126.

[26] Emery, N., Hérold, C., Marêché, J. F., & Lagrange, P. (2008). Synthesis and superconducting properties of CaC6. *Science and Technology of Advanced Materials*, *9*(4), 044102.

[27] Boehm, H. P., Setton, R., & Stumpp, E. (1994). Nomenclature and terminology of graphite intercalation compounds (IUPAC Recommendations 1994). *Pure and Applied Chemistry*, *66*(9), 1893-1901.

[28] Catherine E, Housecroft & Alan G: *Inorganic Chemistry, 3rd Edition*. Pearson. p. 386, chapter 14 (ISBN 978-0-13-175553-6.)

[29] Wang, X., Ouyang, Y., Li, X., Wang, H., Guo, J., & Dai, H. (2008). Room-temperature all-semiconducting sub-10-nm graphene nanoribbon field-effect transistors. *Physical review letters*, *100*(20), 206803.

[30] Jiao, L., Zhang, L., Wang, X., Diankov, G., & Dai, H. (2009). Narrow graphene nanoribbons from carbon nanotubes. *Nature*, *458*(7240), 877-880.

[31] Jepps, N. W., & Page, T. F. (1983). Polytypic transformations in silicon carbide. *Progress in crystal growth and characterization*, *7*(1), 259-307.

[32] Harris, G. L. (Ed.). (1995). *Properties of silicon carbide* (No. 13). Iet.

[33] Suemitsu, M., & Fukidome, H. (2010). Epitaxial graphene on silicon substrates.*Journal of Physics D: Applied Physics*, *43*(37), 374012.

[34] Hüfner, S. (2003). *Photoelectron spectroscopy: principles and applications*. Springer Science & Business Media.

[35] Srivastava, N., He, G., Feenstra, R. M., & Fisher, P. J. (2010). Comparison of graphene formation on C-face and Si-face SiC {0001} surfaces. *Physical Review B*, *82*(23), 235406.

[36] Ferrari, A. C., Meyer, J. C., Scardaci, V., Casiraghi, C., Lazzeri, M., Mauri, F., ... & Geim, A. K. (2006). Raman spectrum of graphene and graphene layers.*Physical review letters*, *97*(18), 187401.

[37] Wang, Y., Alsmeyer, D. C., & McCreery, R. L. (1990). Raman spectroscopy of carbon materials: structural basis of observed spectra. *Chemistry of Materials*,*2*(5), 557-563.

[38] Thomsen, C., & Reich, S. (2000). Double resonant Raman scattering in graphite. *Physical Review Letters*, *85*(24), 5214.

[39] Dresselhaus, M. S., Jorio, A., Hofmann, M., Dresselhaus, G., & Saito, R. (2010). Perspectives on carbon nanotubes and graphene Raman spectroscopy.*Nano letters*, *10*(3), 751-758.

[40] Van Bommel, A. J., Crombeen, J. E., & Van Tooren, A. (1975). LEED and Auger electron observations of the SiC (0001) surface. *Surface Science*, *48*(2), 463-472.

[41] Forbeaux, I., Themlin, J. M., & Debever, J. M. (1998). Heteroepitaxial graphite on 6 H-SiC (0001): Interface formation through conduction-band electronic structure. *Physical Review B*, *58*(24), 16396.

[42] Van Elsbergen, V., Kampen, T. U., & Mönch, W. (1996). Surface analysis of 6H□ SiC. *Surface science*, *365*(2), 443-452.

[43] Riedl, C., Coletti, C., & Starke, U. (2010). Structural and electronic properties of epitaxial graphene on SiC (0 0 0 1): a review of growth, characterization, transfer doping and hydrogen intercalation. *Journal of Physics D: Applied Physics*, *43*(37), 374009.

[44] Geim, A. K. (2009). Graphene: status and prospects. *science*, *324*(5934), 1530-1534.

[45] Peres, N. M. R., Yang, L., & Tsai, S. W. (2009). Local density of states and scanning tunneling currents in graphene. *New Journal of Physics*, *11*(9), 095007.

[46] Jeans, J. H. (1982). *An introduction to the kinetic theory of gases*. CUP Archive.

[47] GEIM, A. K., & MACDONALD, A. H. (2007). Graphene: Exploring corbon flotland. *Physics today*, *60*(8), 35-41